Experimental and DFT Studies of Cationic Imido Titanium Alkyls: Agostic Interactions and C−H Bond and Solvent Activation Reactions of Isolobal Analogues of Group 4 Metallocenium Cations

Paul D. Bolton,[†] Eric Clot,*[,‡] Nico Adams,[†] Stuart R. Dubberley,[†] Andrew R. Cowley,[†] and Philip Mountford*[,†]

Chemistry Research Laboratory, University of Oxford, Mansfield Road, Oxford OX1 3TA, U.K., and LSDSMS (UMR CNRS 5636), Institut Charles Gerhardt, cc 14, Université Montpellier 2, 34095 Montpellier Cedex 5, France

Received January 31, 2006

Synthesis, reactions, and DFT studies of macrocycle-supported imido titanium alkyl cations derived from Ti(N^{t}Bu)(Me$_3$[9]aneN$_3$)R$_2$ (R = Me (**1**) or CH$_2$SiMe$_3$ (**2**)) are described (Me$_3$[9]aneN$_3$ = 1,4,7-trimethyltriazacyclononane). Reaction of **1** with 1 equiv of [Ph$_3$C][BAr$^F_4$] or BAr$^F_3$ (Ar^F = C$_6$F$_5$) in C$_6$D$_5$Br afforded the methyl cation [Ti(N^{t}Bu)(Me$_3$[9]aneN$_3$)Me]$^+$ (**6**$^+$), whereas with half an equivalent of [Ph$_3$C][BAr$^F_4$] the fluxional methyl-bridged homo-binuclear cation [Ti$_2$(N^{t}Bu)$_2$(Me$_3$[9]aneN$_3$)$_2$Me$_2$(μ-Me)]$^+$ (**10**$^+$) was formed. Reaction of **1** with [Ph$_3$C][BAr$^F_4$] in CD$_2$Cl$_2$ formed the monochloride cation [Ti(N^{t}Bu)(Me$_3$[9]aneN$_3$)Cl]$^+$ (**8**$^+$), which was also prepared from Ti(N^{t}Bu)(Me$_3$[9]aneN$_3$)Cl(Me) and [Ph$_3$C][BAr$^F_4$]. Cation **8**$^+$ reacted with pyridine to give the adduct [Ti(N^{t}Bu)(Me$_3$[9]aneN$_3$)Cl(py)]$^+$ (**9**$^+$) and with Ti(N^{t}Bu)(Me$_3$[9]aneN$_3$)Me$_2$ to form the chloride-bridged cation [Ti$_2$(N^{t}Bu)$_2$(Me$_3$[9]aneN$_3$)$_2$-Me$_2$(μ-Cl)]$^+$ (**11**$^+$). Reaction of **2** with [Ph$_3$C][BAr$^F_4$] gave [Ti(N^{t}Bu)(Me$_3$[9]aneN$_3$)(CH$_2$SiMe$_3$)]$^+$ (**7**$^+$), which is stabilized by a β-Si−C agostic interaction characterized by a high-field-shifted ^{29}Si NMR resonance. Attempts to generate **7**$^+$ by reaction of **2** with [PhNMe$_2$H][BAr$^F_4$] in CH$_2$Cl$_2$ led to Ti(N^{t}Bu)(Me$_3$[9]aneN$_3$)Cl$_2$ and [PhNMe$_2$(CH$_2$Cl)][BAr$^F_4$] (**12-BAr$^F_4$**) via a series of solvent activation reactions, the details of which have been elucidated. Reaction of **6**$^+$ or **7**$^+$ with Ph$_3$PO afforded the adducts [Ti(N^{t}Bu)(Me$_3$[9]aneN$_3$)R(Ph$_3$PO)]$^+$, whereas with pyridine a C−H bond activation reaction occurred to give [Ti(N^{t}Bu)(Me$_3$[9]aneN$_3$)(NC$_5$H$_4$)]$^+$ (**17**$^+$) and the corresponding alkane RH. Density functional theory calculations of the isolobal d^0 fragments [Ti(NR)(R′$_3$[9]aneN$_3$)]$^{2+}$ and [Cp$_2$Ti]$^{2+}$ found that their frontier orbitals, although broadly similar, featured important differences in their shapes and energies. These account for the absence of any α-C−H agostic interaction in **6**$^+$, whereas [Cp$_2$TiMe]$^+$ is stabilized by a weak interaction of this type, as judged by DFT-computed geometries. The experimentally observed increase in Ti−Me group average $^1J_{CH}$ on forming either **6**$^+$ from **1** or [Cp$_2$TiMe]$^+$ from Cp$_2$TiMe$_2$ is reproduced by DFT and attributed to intrinsic global changes in carbon 2s orbital contribution to the Ti−C and C−H bonds upon cation formation. These changes were shown to mask the otherwise expected decrease in average $^1J_{CH}$ for the α-agostic methyl in [Cp$_2$TiMe]$^+$. The difference between the Ti−Me $^1J_{CH}$ values in **1** (111 Hz) and isolobal Cp$_2$TiMe$_2$ (124 Hz) was also attributed to differences in Ti center electrophilicity. The experimental high-field-shifted ^{29}Si NMR resonance in **7**$^+$ was well reproduced in the DFT-computed β-Si−C agostic structure, and upper and lower limits for the strength of the agostic interaction were estimated. An NBO analysis of the Ti−CH$_2$SiMe$_3$ bonding found several different contributions, including negative hyperconjugation (population of σ^*(Si$_\beta$−C$_\gamma$)) and formal C$_\alpha$−Si$_\beta$→Ti and Si$_\beta$−C$_\gamma$→Ti bond pair donation.

Introduction

Homogeneous group 4 metallocene,[1−5] constrained geometry,[6] and a wide variety of "post-metallocene"[7−10] Ziegler−Natta type olefin polymerization catalysts have been a continuing focus of academic and industrial interest. Of particular relevance to this contribution is the ability of certain transition metal imido compounds (general type L$_n$M═NR) to act as olefin polymerization catalysts.[11] The first catalysts of this type were bis(imido)chromium dichloride and dialkyl compounds Cr(NR)$_2$X$_2$ (R = ^{t}Bu or 2,6-C$_6$H$_3$^{i}Pr$_2$; X = Cl, Me, or CH$_2$Ph),[12,13] and activities of up to 66 kg(PE) mol^{-1} h^{-1} bar^{-1} were reported.

* To whom correspondence should be addressed. E-mail: eric.clot@univ-montp2.fr; philip.mountford@chem.ox.ac.uk.
† University of Oxford.
‡ LSDSMS.

(1) Bochmann, M. *J. Chem. Soc., Dalton Trans.* **1996**, 255.
(2) Brintzinger, H. H.; Fischer, D.; Mülhaupt, R.; Rieger, B.; Waymouth, R. M. *Angew. Chem., Int. Ed. Engl.* **1995**, *34*, 1143.
(3) Janiak, C. In *Metallocenes: Synthesis, Reactivity, Applications*; Togni, A., Halterman, R. L., Eds.; Wiley-VCH: New York, 1998; Vol. 2.
(4) Kaminsky, W. *J. Chem. Soc., Dalton Trans.* **1998**, 1413.
(5) Bochmann, M. *J. Organomet. Chem.* **2004**, *689*, 3982.
(6) McKnight, A. L.; Waymouth, R. M. *Chem. Rev.* **1998**, *98*, 2587.
(7) Britovsek, G. J. P.; Gibson, V. C.; Wass, D. F. *Angew. Chem., Int. Ed.* **1999**, *38*, 429.
(8) Gibson, V. C.; Spitzmesser, S. K. *Chem. Rev.* **2003**, *103*, 283.
(9) Suzuki, Y.; Terao, H.; Fujita, T. *Bull. Chem. Soc. Jpn.* **2003**, *76*, 1493.
(10) Mitani, M.; Saito, J.; Ishii, S.; Nakayama, Y.; Makio, H.; Matsukawa, N.; Matsui, S.; Mohri, J.; Furuyama, R.; Terao, H.; Bando, H.; H., T.; Fujita, T. *Chem. Rec.* **2004**, *4*, 137.
(11) Bolton, P. D.; Mountford, P. *Adv. Synth. Catal.* **2005**, *347*, 355.

10.1021/om060096r CCC: $33.50
Publication on Web 04/21/2006

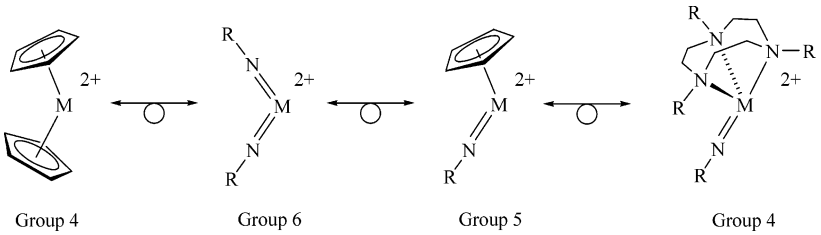

Figure 1. Isolobal relationships between d^0 fragments in transition metal imido chemistry.

NMR evidence for the monobenzyl cation $[Cr(N^tBu)_2(\eta^2\text{-}CH_2Ph)]^+$ (a proposed initiating species in olefin polymerization by $Cr(N^tBu)_2(CH_2Ph)_2$) was advanced and a PMe_3 adduct identified also by NMR. A notable feature of group 6 bis(imido) and group 5 cyclopentadienyl-imido catalysts of the type $M(NR)_2X_2$ and $CpM(NR)X_2$, respectively, is their isolobal relationship[14] with the group 4 metallocene-derived systems Cp_2MX_2. This arises from the relationships summarized in Figure 1 for $[Cp_2M]^{2+}$ (M = group 4), $[CpM(NR)]^{2+}$ (group 5), and $[M(NR)_2]^{2+}$ (group 6), as has been discussed and documented elsewhere.[15−18]

As part of our broad program in titanium imido chemistry,[19−21] we have targeted compounds of the type $Ti(NR)(\textit{fac}\text{-}L_3)Cl_2$ (*fac*-L_3 = triazacyclohexane,[22] triazacyclononane,[23−25] tris-(3,5-dimethylpyrazolyl)methane;[26,27] (NR)(*fac*-L_3) = *ansa*-type κ^4 -coordinated macrocycle-imido ligand[23]) as potential polymerization catalysts. We recently reported a library of ca. 50 1,4,7-trimethyl triazacyclononane ($Me_3[9]aneN_3$)-supported imido titanium catalysts $Ti(NR)(Me_3[9]aneN_3)Cl_2$ in which the imido N−R substitutent was varied.[28] Some of these were the most active imido-based Ziegler−Natta polymerization catalysts reported to date, with ethylene polymerization productivities of up to 10^5 kg(PE) mol^{-1} h^{-1} bar^{-1}. Furthermore, since both a six-electron-donor imido dianion NR^{2-} and a neutral conical *fac*-L_3 donor[29] such as $Me_3[9]aneN_3$ are isolobal with the $C_5H_5^-$ monoanion, the compounds $Ti(NR)(Me_3[9]aneN_3)Cl_2$ are also isolobal analogues of the group 4 metallocenes Cp_2MCl_2 (Figure 1).

We have also shown that activation of the dialkyls $Ti(N^tBu)(Me_3[9]aneN_3)R_2$ (R = Me (**1**) or CH_2SiMe_3 (**2**)) with $[Ph_3C][BAr^F{}_4]$ ($Ar^F = C_6F_5$) gives highly active catalysts for ethylene polymerization, presumably through the formation of the corresponding alkyl cations $[Ti(N^tBu)(Me_3[9]aneN_3)R]^+$.[28] Surprisingly, although a great deal is known about metallocenium and nonmetallocenium alkyl cations (widely accepted as being the active species in Ziegler−Natta olefin polymerization),[5,30] little has been reported about imido-supported alkyl cations,[28,31−34] or indeed cationic imido compounds in general.[25,35−40] In this contribution we describe the synthesis, properties, and Lewis base adducts of *tert*-butyl imido titanium monoalkyl cations, along with detailed DFT studies of them and comparisons with the bis(cyclopentadienyl) isolobal analogue $[Cp_2TiMe]^+$. Part of this work has been communicated.[41]

Results and Discussion

Reactions of $Ti(N^tBu)(Me_3[9]aneN_3)R_2$ (R = Me (1) or CH_2SiMe_3 (2)) with $BAr^F{}_3$ or $[Ph_3C][BAr^F{}_4]$. The dialkyl compounds $Ti(N^tBu)(Me_3[9]aneN_3)R_2$ (R = Me (**1**) or CH_2SiMe_3 (**2**)) were prepared as described.[28] The new monoalkylmonochloride $Ti(N^tBu)(Me_3[9]aneN_3)Cl(CH_2SiMe_3)$ (**3**) was prepared from **2** and Ph_3CCl[42] (41% recrystallized yield) since the reaction of $Ti(N^tBu)(Me_3[9]aneN_3)Cl_2$ (**4**)[24] with 1 equiv of $LiCH_2SiMe_3$ gave a mixture of **2** and **3**, which could not be separated by fractional crystallization. The reactions of **1** and **2** with $BAr^F{}_3$ and $[Ph_3C][BAr^F{}_4]$ ($Ar^F = C_6F_5$) (commonly used reagents for alkyl anion abstraction[43−45]) are summarized in

(12) Coles, M. P.; Dalby, C. I.; Gibson, V. C.; Clegg, W.; Elsegood, M. R. J. *J. Chem. Soc., Chem. Commun.* **1995**, 1709.
(13) Coles, M. P.; Dalby, C. I.; Gibson, V. C.; Little, I. R.; Marshall, E. L.; Ribeiro da Costa, M. H.; Mastroianni, S. *J. Organomet. Chem.* **1999**, *591*, 78.
(14) Hoffmann, R. *Angew. Chem., Int. Ed. Engl.* **1982**, *21*, 711.
(15) Williams, D. S.; Schofield, M. H.; Anhaus, J. T.; Schrock, R. R. *J. Am. Chem. Soc.* **1990**, *112*, 6728.
(16) Glueck, D. S.; Green, J. C.; Michelman, R. I.; Wright, I. N. *Organometallics* **1992**, *11*, 4221.
(17) Williams, D. S.; Schofield, M. H.; Schrock, R. R. *Organometallics* **1993**, *12*, 4560.
(18) Gibson, V. C. *J. Chem. Soc., Dalton Trans.* **1994**, 1607.
(19) Gade, L. H.; Mountford, P. *Coord. Chem. Rev.* **2001**, *216−217*, 65.
(20) Hazari, N.; Mountford, P. *Acc. Chem. Res.* **2005**, *38*, 839.
(21) Mountford, P. *Chem. Commun.* **1997**, 2127.
(22) Wilson, P. J.; Blake, A. J.; Mountford, P.; Schröder, M. *J. Organomet. Chem.* **2000**, *600*, 71.
(23) Male, N. A. H.; Skinner, M. E. G.; Bylikin, S. Y.; Wilson, P. J.; Mountford, P.; Schröder, M. *Inorg. Chem.* **2000**, *39*, 5483.
(24) Wilson, P. J.; Blake, A. J.; Mountford, P.; Schröder, M. *Chem. Commun.* **1998**, 1007.
(25) Gardner, J. D.; Robson, D. A.; Rees, L. H.; Mountford, P. *Inorg. Chem.* **2001**, *40*, 820.
(26) Lawrence, S. C.; Skinner, M. E. G.; Green, J. C.; Mountford, P. *Chem. Commun.* **2001**, 705.
(27) Bigmore, H. R.; Dubberley, S. R.; Kranenburg, M.; Lawrence, S. C.; Sealey, A. J.; Selby, J. D.; Zuideveld, M.; Cowley, A. R.; Mountford, P. *Chem. Commun.* **2006**, 436.
(28) Adams, N.; Arts, H. J.; Bolton, P. D.; Cowell, D.; Dubberley, S. R.; Friederichs, N.; Grant, C.; Kranenburg, M.; Sealey, A. J.; Wang, B.; Wilson, P. J.; Cowley, A. R.; Mountford, P.; Schröder, M. *Chem. Commun.* **2004**, 434.
(29) Elian, M.; Chen, M. M. L.; Mingos, D. M. P.; Hoffmann, R. *Inorg. Chem.* **1976**, *15*, 1148.
(30) Jordan, R. F. *Adv. Organomet. Chem.* **1991**, *32*, 325.
(31) Ward, B. D.; Clot, E.; Dubberley, S. R.; Gade, L. H.; Mountford, P. *Chem. Commun.* **2002**, 2618.
(32) Ward, B. D.; Orde, G.; Clot, E.; Cowley, A. R.; Gade, L. H.; Mountford, P. *Organometallics* **2004**, *23*, 4444.
(33) Anderson, L. L.; Arnold, J.; Bergman, R. G. *Org. Lett.* **2004**, *15*, 2519.
(34) Ward, B. D.; Orde, G.; Clot, E.; Cowley, A. R.; Gade, L. H.; Mountford, P. *Organometallics* **2005**, *24*, 2368.
(35) Danopoulos, A. A.; Wilkinson, G.; Sweet, T. K. N.; Hursthouse, M. B. *J. Chem. Soc., Dalton Trans.* **1995**, 937.
(36) Witte, P. T.; Meetsma, A.; Hessen, B.; Budzelaar, P. H. M. *J. Am. Chem. Soc.* **1997**, *119*, 10561.
(37) Blake, R. E.; Antonelli, D. M.; Henling, L. M.; Schaefer, W. P.; Hardcastle, K. I.; Bercaw, J. E. *Organometallics* **1998**, *17*, 718.
(38) Chan, M. C. W.; Lee, F. W.; Cheung, K. K.; Che, C. M. *Dalton Trans.* **1999**, 3197.
(39) Sceats, E. L.; Figueroa, J. S.; Cummins, C. C.; Loening, N. M.; Van der Wel, P.; Griffin, R. G. *Polyhedron* **2004**, *23*, 2751.
(40) Basuli, F.; Clark, R. L.; Bailey, B. C.; Brown, D.; Huffman, J. C.; Mindiola, D. J. *Chem. Commun.* **2005**, 2250.
(41) Bolton, P. D.; Clot, E.; Cowley, A. R.; Mountford, P. *Chem. Commun.* **2005**, 3313.
(42) Hawrelak, E. J.; Deck, P. A. *Organometallics* **2004**, *23*, 9.
(43) Chen, E. Y.-X.; Marks, T. J. *Chem. Rev.* **2000**, *100*, 1391.
(44) Bochmann, M.; Lancaster, S. J.; Hannant, M. D.; Rodriguez, A.; Schormann, M.; Walker, D. A.; Woodman, T. J. *Pure Appl. Chem.* **2003**, *75*, 1183.
(45) Piers, W. E. *Adv. Organomet. Chem.* **2005**, *52*, 1.

Scheme 1. Reactions of Ti(N^{t}Bu)(Me$_3$[9]aneN$_3$)R$_2$ (R = Me or CH$_2$SiMe$_3$) and Ti(N^{t}Bu)(Me$_3$[9]aneN$_3$)Cl(Me) with BAr$^F_3$ or [Ph$_3$C][BAr$^F_4$]^a

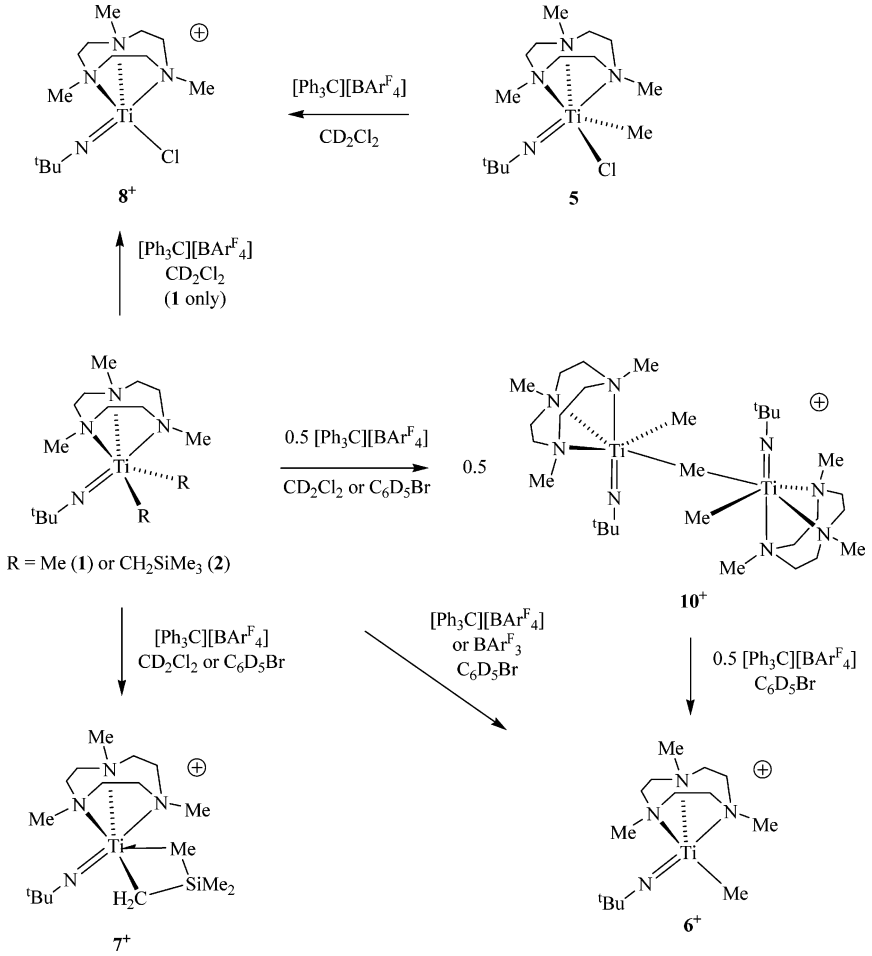

[a] Anions omitted for clarity.

Scheme 1. Complementary studies with the previously described Ti(N^{t}Bu)(Me$_3$[9]aneN$_3$)Cl(Me) (**5**)[46] are shown in Schemes 1 and 3.

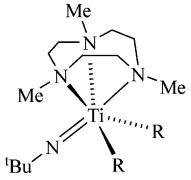

Reaction of **1** or **2** with [Ph$_3$C][BAr$^F_4$] in C$_6$D$_5$Br quantitatively formed well-defined monoalkyl cations [Ti(N^{t}Bu)(Me$_3$[9]aneN$_3$)Me]$^+$ (**6**$^+$) and [Ti(N^{t}Bu)(Me$_3$[9]aneN$_3$)(CH$_2$SiMe$_3$)]$^+$ (**7**$^+$), respectively, on an NMR tube scale. The nature of the organic side-product "Ph$_3$CCH$_2$SiMe$_3$" formed in the synthesis of **7**$^+$ is discussed below. Although reasonably stable in solution at room temperature, these coordinatively unsaturated, formally 14 valence electron species could be isolated only as adducts (see below). The ^{19}F NMR spectra showed no evidence for coordination of the [BAr$^F_4$]$^-$ counteranion. Reaction of **2** with [Ph$_3$C][BAr$^F_4$] in CD$_2$Cl$_2$ also afforded **7**$^+$. Remarkably, these solutions remained unchanged for several *days* at room temperature, whereas reaction of **1** with either BAr$^F_3$ or [Ph$_3$C][BAr$^F_4$] in CD$_2$Cl$_2$ instantaneously gave the monochloride cation [Ti(N^{t}Bu)(Me$_3$[9]aneN$_3$)Cl]$^+$ (**8**$^+$). Reaction of **1** with BAr$^F_3$ in C$_6$D$_5$Br also cleanly gave **6**$^+$ and the expected counteranion side-product [MeBAr$^F_3$]$^-$. Surprisingly, reaction of **2** with BAr$^F_3$ in either C$_6$D$_5$Br or CD$_2$Cl$_2$ gave ill-defined mixtures. The NMR spectra of **6**$^+$ were independent of the counteranion (i.e., either [BAr$^F_4$]$^-$ or [MeBAr$^F_3$]$^-$), and neither the ^{1}H nor ^{19}F NMR data for the [MeBAr$^F_3$]$^-$ anion in **6-MeBAr$^F_3$** showed any evidence for significant interaction with the cation.[47] It is possible, however, that one or both of the cations **6**$^+$ and **7**$^+$ are weakly stabilized by halogenated solvent coordination.[36,48−53]

The formation of [Ti(N^{t}Bu)(Me$_3$[9]aneN$_3$)Me]$^+$ (**6**$^+$) from **1** and [Ph$_3$C][BAr$^F_4$] was accompanied by the expected Ph$_3$CMe organic side-product. Unexpectedly, however, the ^{1}H and ^{29}Si NMR and other data for the organic side-product "Me$_3$SiCH$_2$CPh$_3$" formed in the synthesis of **7**$^+$ from **2** and [Ph$_3$C][BAr$^F_4$] were more complicated than expected for a single

(46) Wilson, P. J. Ph.D. Thesis, Nottingham University, 1999.

(47) Horton, A. D.; de With, J.; van der Linden, A. J.; van de Weg, H. *Organometallics* **1996**, *15*, 2672.

(48) Kulawiec, R. J.; Faller, J. W.; Crabtree, R. H. *Organometallics* **1990**, *9*, 745.

(49) Butts, M. D.; Scott, B. L.; Kubas, G. J. *J. Am. Chem. Soc.* **1996**, *118*, 11831.

(50) Hayes, P. G.; Piers, W. E.; Parvez, M. *J. Am. Chem. Soc.* **2003**, *125*, 5622.

(51) Stoebenau, E. J.; Jordan, R. F. *J. Am. Chem. Soc.* **2003**, *125*, 3222.

(52) Wu, F.; Dash, A. K.; Jordan, R. F. *J. Am. Chem. Soc.* **2004**, *126*, 15360.

(53) Bouwkamp, M. W.; Budzelaar, P. H. M.; Gercama, J.; Del Hierro Morales, I.; Meetsma, A.; Troyanov, S. I.; Teuben, J. H.; Hessen, B. *J. Am. Chem. Soc.* **2005**, *127*, 14310.

Scheme 2. Likely Fluxional Processes for $[Ti(N^tBu)(Me_3[9]aneN_3)(CH_2SiMe_3)]^+$

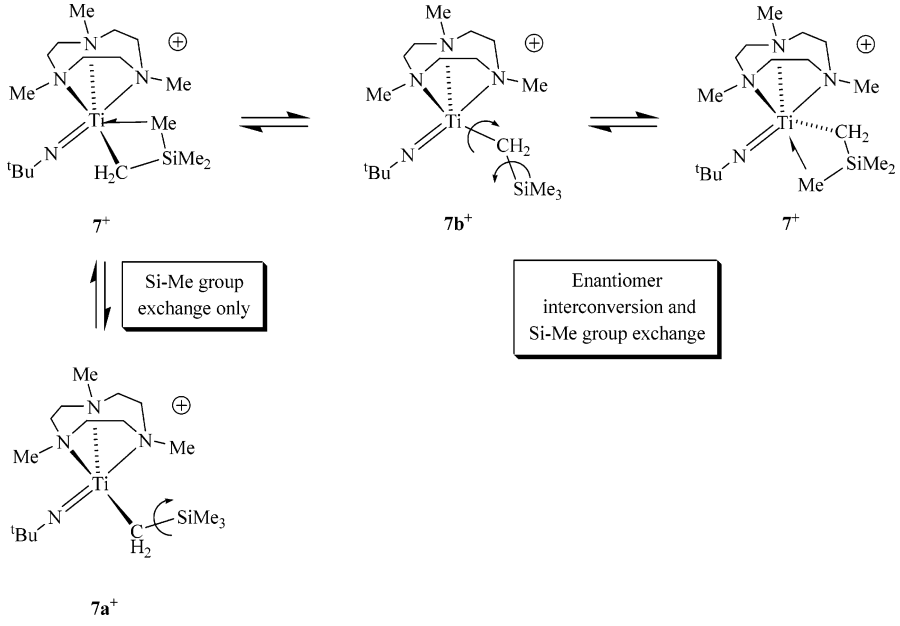

7^+ $7b^+$ 7^+ $7a^+$

Scheme 3. Reaction of$Ti(N^tBu)(Me_3[9]aneN_3)Cl(Me)$ with $[Ph_3C][BAr^F_4]$ and Subsequent Trapping of the in Situ-Generated $[Ti(N^tBu)(Me_3[9]aneN_3)Cl]^+$ Cation[a]

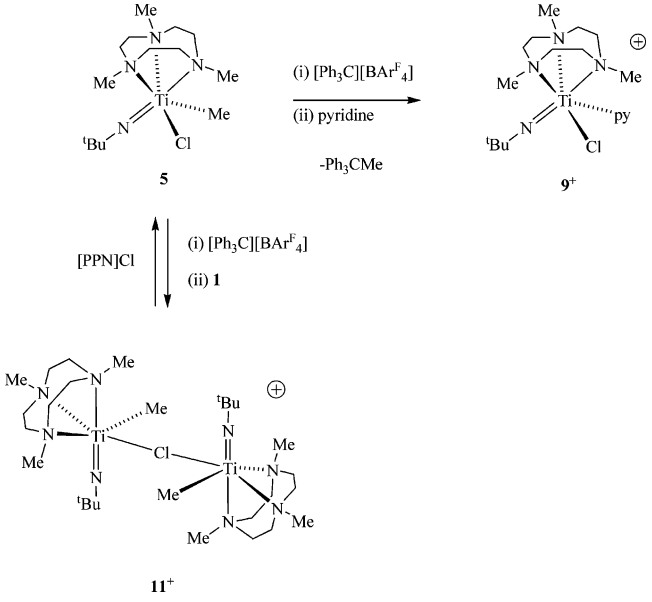

5 9^+ 11^+

[a] Anions omitted for clarity.

species. Thus (in addition to the resonances for 7^+) the ^1H NMR spectrum of the reaction mixture featured *two* singlets at −0.01 and −0.32 ppm (the expected region for $SiMe_3$ resonances) and *two* methylene resonances at 2.12 and 2.06 ppm. The ratio of the $SiMe_3$ to methylene resonance intensities for each of the two presumed isomers of "$Me_3SiCH_2CPh_3$" was 9:2. The ^1H resonances for each isomer correlated (via a $^1H-^{29}Si$ HMQC (^1H-observed) NMR spectrum) to two ^{29}Si resonances at 0.7 and −1.1 ppm. The ratio of the two isomers of "$Me_3SiCH_2CPh_3$" was ca. 2:1. In addition there was also always a small amount of Ph_3CH formed (ca. 15% by integration compared to "$Me_3SiCH_2CPh_3$").

In an attempt to better understand these products, the reaction of $LiCH_2SiMe_3$ with Ph_3CCl in benzene was carried out. This yielded a yellow oil having NMR spectra comparable to those of organic side-products from the reaction of **2** and $[Ph_3C][BAr^F_4]$. Neither a high-vacuum, short-path distillation nor preparative scale HPLC experiment was able to separate the components of the mixture, which was therefore analyzed by GC-MS. This confirmed the presence of three species in the mixture. In order of elution, the first fraction was identified as Ph_3CH in accordance with the ^1H and ^{13}C NMR spectra. The second and third fractions both gave parent ion peaks at *m*/*z* 330, corresponding to "$[Me_3SiCH_2CPh_3]^+$". Although the fragmentation patterns of each isomer were somewhat different, most of the fragments could not be identified.

The trigonal bipyramidal structure shown for $\mathbf{6}^+$ in Scheme 1 is supported by DFT calculations presented below. The ^1H NMR spectrum of $\mathbf{6}^+$ in C_6D_5Br revealed that this five-coordinate cation is highly fluxional at room temperature. The Ti−Me and *tert*-butyl groups appeared as sharp singlets, whereas the macrocycle methyl groups appeared as a single broad resonance (9 H) and the methylene protons as two broad multiplets of relative intensity 6 H each. The presence of two sets of methylene resonances (i.e., "up" and "down" with respect to the metal) confirms that the ligand remains bound to the cationic metal center, but that there is a rapid exchange of all three N-donor sites on the NMR time scale. Cooling to 248 K resulted in a broadening of the macrocycle resonances (the Ti−Me and *tert*-butyl groups remaining as sharp singlets), but a slow exchange limiting spectrum could not be obtained before the freezing point of the solvent was reached.

Since $\mathbf{6}^+$ is a 14 valence electron monomethyl cation, this suggests the possibility of α-C−H agostic interactions between the Ti−Me hydrogens and the metal center.[54−56] Interestingly, however, the Ti−Me $^1J_{CH}$ coupling constant *increases* slightly from 111 Hz in the dimethyl precursor **1** (also in C_6D_5Br) to 116 Hz in $\mathbf{6}^+$. We note that the methyl titanocenium system $[Cp_2TiMe][MeBAr^F_3]$ has been reported to display an α-agostic interaction on the basis of vibrational spectroscopic studies.[56] For comparison with the data for **1** and $\mathbf{6}^+$ we measured $^1J_{CH}$ for the Ti−Me groups in Cp_2TiMe_2 (124 Hz) and $[Cp_2TiMe][BAr^F_4]$ (129 Hz) in C_6D_5Br. There is again a small increase in

(54) Brookhart, M.; Green, M. L. H.; Wong, L.-L. *Prog. Inorg. Chem.* **1988**, *36*, 1.
(55) Clot, E.; Eisenstein, O. *Struct. Bond.* **2004**, *113*, 1.
(56) Scherer, W.; McGrady, G. S. *Angew. Chem., Int. Ed.* **2004**, *43*, 1782.

$^1J_{CH}$ on going from the neutral dimethyl species to the corresponding monomethyl cation. Furthermore, both Cp_2TiMe_2 and $[Cp_2TiMe]^+$ possess $^1J_{CH}$ values that are 13 Hz greater than in the macrocycle-imido analogues. Grubbs has shown previously that small changes in average Ti−Me group $^1J_{CH}$ values can in principle be attributed to changes in the effective electronegativity of a metal center.[57] The electronic and molecular structures of macrocycle-imido and bis(cyclopentadienyl) titanium methyl compounds are addressed by DFT later on.

The trimethylsilylmethyl cation $\mathbf{7}^+$ is also fluxional on the NMR time scale at room temperature, but in this case the fluxional process(es) can be partially "frozen out". Cooling a CD_2Cl_2 sample to 213 K led to the observation of two macrocycle NMe groups (relative ratio 6 H:3 H, attributed to those lying *cis* and *trans* to the N^{t}Bu ligand, respectively). The CH_2SiMe_3 ligand methylene and methyl groups still appeared as broad singlets at 213 K. Notably, the ^{29}Si chemical shift for $\mathbf{7}^+$ in CD_2Cl_2 (−15.9 ppm) or C_6D_5Br (−17.5 ppm) is significantly upfield from that of the neutral dialkyl **2** (−1.8 ppm in CD_2Cl_2 or −3.1 ppm in C_6D_5Br). A comparison can also be made with the monoalkyl-monochloride Ti(N^{t}Bu)(Me$_3$[9]aneN$_3$)Cl(CH$_2$SiMe$_3$) (**3**), the ^{29}Si shift of which appears at −1.8 ppm in CD_2Cl_2. Horton has reported[58] cationic zirconium vinyl compounds (e.g., $[Cp_2Zr\{C(=CMe_2)SiMe_3\}]^+$) that possess agostic Si−Me···Zr interactions (supported in one case by X-ray crystallography) and have associated high-field-shifted ^{29}Si resonances. Eisch has structurally characterized a similar compound for a titanocenium system, but no ^{29}Si NMR data were presented.[59]

Si−Me···M interactions are fairly widespread, especially in neutral group 3 and lanthanide systems, notably for compounds with $CH(SiMe_3)_2$ or $N(SiMe_3)_2$ ligands.[55,56,60] With regard to cationic group 4 silyl-alkyl systems we note that Eisch has advanced spectroscopic evidence for the titanocene trimethylsilylmethyl cation $[Cp_2TiCH_2SiMe_3]^+$ as part of an ion pair with $[AlCl_4]^-$.[61] Marks has reported that $SiMe_3$ group exchange can be "frozen out" at low temperature for the bulky $CH(SiMe_3)_2$ ligand in the cation $[(\eta\text{-}C_5H_3Me_2)_2Zr\{CH(SiMe_3)_2\}]^+$ and has attributed this to either steric congestion or an agostic interaction.[62] Very recently, Bochmann, Macchioni, and co-workers attributed the restricted $SiMe_3$ group rotation in the cations $[\{rac\text{-}Me_2Si(1\text{-Indenyl})_2\}MCH_2SiMe_3]^+$ (M = Zr or Hf)[63] to an agostic interaction of one of the methyl groups with the metal centers. For M = Hf in this latter system the $SiMe_3$ rotation could be "frozen out", whereas for M = Zr the slow exchange limit could not be reached.[63] In none of these cases were ^{29}Si NMR data reported.

The presence of an otherwise 14 valence electron center in $\mathbf{7}^+$ would provide a driving force for the β-Si−C···Ti$^+$ interaction depicted in Scheme 1, and the upfield ^{29}Si NMR shift appears to be consistent with this. However, a static C_1 symmetric structure of the type illustrated should lead to three independent macrocycle ligand methyl group resonances of equal intensity and also to three different Si−Me resonances. The broad spectrum suggesting C_s symmetry observed at 213 K implies that the β-Si−C agostic interaction is rather weak and that the likely fluxional processes shown in Scheme 2 (enantiomer interconversion and/or $SiMe_3$ methyl group exchange) have low activation energies. However, the fact that $\mathbf{7}^+$ is fairly stable in CD_2Cl_2 (whereas the methyl cation $\mathbf{6}^+$ is not) suggests that the β-Si−C···Ti interaction (possibly in conjunction with increased steric protection) nevertheless provides a significant stabilizing effect. DFT studies of $\mathbf{7}^+$ and models of the possible transition states/intermediates $\mathbf{7a}^+$ and $\mathbf{7b}^+$ are described below.

Further experiments confirmed the identity of $\mathbf{8}^+$ as the monochloride cation $[Ti(N^tBu)(Me_3[9]aneN_3)Cl]^+$. The NMR tube scale reaction of Ti(N^{t}Bu)(Me$_3$[9]aneN$_3$)Cl(Me) (**5**) with $[Ph_3C][BAr^F_4]$ gave clean conversion to $\mathbf{8}^+$ and Ph_3CMe. Samples of $\mathbf{8}^+$ made in this way have ^{1}H NMR spectra identical to those generated above from **1** and $[Ph_3C][BAr^F_4]$ in CD_2Cl_2. Like $[Ti(N^tBu)(Me_3[9]aneN_3)Me]^+$ ($\mathbf{6}^+$), five-coordinate $\mathbf{8}^+$ is highly fluxional at room temperature, with the three macrocycle methyl groups and the methylene resonances appearing as a series of broad multiplets, while the *tert*-butyl group appears as a sharp singlet. Unlike $\mathbf{6}^+$, however, the low-temperature (213 K) spectrum showed the presence of several *tert*-butyl and macrocycle environments. This suggests some degree of dimerization or other aggregation (possibly via μ-Cl or/and μ-N^{t}Bu bridges) at lower temperatures. We note that the neutral and isolobal analogue "CpTi(N^{t}Bu)Cl" exists as an imido-bridged dimer $Cp_2Ti_2(\mu\text{-}N^tBu)_2Cl_2$ in the solid state[64] and that the chloride-bridged cyclopentadienyl-phosphinimide dication $[Cp_2Ti_2(NP^tBu_3)_2(\mu\text{-}Cl)_2]^{2+}$ has recently been structurally characterized.[65] Regardless of the presence of different species present in solution, addition of pyridine to NMR samples of $\mathbf{8}^+$ gave complete conversion to a single product, namely, the C_1-symmetric, nonfluxional cation $[Ti(N^tBu)(Me_3[9]aneN_3)Cl(py)]^+$ ($\mathbf{9}^+$), as indicated by sharp resonances for a nonsymmetric $Me_3[9]aneN_3$ ligand, a terminal *tert*-butyl imido ligand, and a coordinated pyridine. The compound **9-BAr$^F_4$** was isolated on the preparative scale as an orange crystalline solid in 81% yield (Scheme 3), and its X-ray crystal structure has been determined.

The molecular structure of $[Ti(N^tBu)(Me_3[9]aneN_3)Cl(py)]^+$ ($\mathbf{9}^+$) is shown in Figure 2, and selected distances and angles are listed in Table 1. The structure is in agreement with the NMR data, and the bond lengths and angles around titanium and associated with the ligands themselves are within the expected ranges.[66,67] There are no unusually close contacts between the cation and the $[BAr^F_4]^-$ anion. The Ti−Cl and Ti−N distances are all slightly shorter than the corresponding ones in the neutral dichloride Ti(N^{t}Bu)(Me$_3$[9]aneN$_3$)Cl$_2$ (**4**),[24] as would be expected from the cationic nature of $\mathbf{9}^+$.

Methyl- and Chloride-Bridged Homobimetallic Cations. Reaction of dimethyl compound **1** with 0.5 equiv of $[Ph_3C][BAr^F_4]$ in C_6D_5Br gave the cationic, methyl-bridged dinuclear species $[Ti_2(N^tBu)_2(Me_3[9]aneN_3)_2Me_2(\mu\text{-}Me)]^+$ ($\mathbf{10}^+$, Scheme 1). Reaction with a further half equivalent of $[Ph_3C][BAr^F_4]$ gave $\mathbf{6}^+$. Interestingly, $\mathbf{10}^+$ can also be generated in CD_2Cl_2, in which it is moderately stable (unlike $\mathbf{6}^+$, which immediately forms $\mathbf{8}^+$). The cation $\mathbf{10}^+$ is fluxional at room temperature,

(57) Finch, W. C.; Anslyn, E. V.; Grubbs, R. H. *J. Am. Chem. Soc.* **1988**, *110*, 2406.
(58) Horton, A. D.; Orpen, A. G. *Organometallics* **1991**, *10*, 3910.
(59) Eisch, J. J.; Piotrowski, A. M.; Brownstein, S. K.; Gabe, E. J.; Lee, F. L. *J. Am. Chem. Soc.* **1985**, *107*, 7219.
(60) Nikonov, G. I. *J. Organomet. Chem.* **2001**, *635*, 24.
(61) Eisch, J. J.; Caldwell, K. R.; Werner, S.; Kruger, C. *Organometallics* **1991**, *10*, 3417.
(62) Beswick, C. L.; Marks, T. J. *J. Am. Chem. Soc.* **2000**, *122*, 10358.
(63) Song, F.; Lancaster, S. J.; Cannon, R. D.; Schormann, M.; Humphrey, S. M.; Zuccaccia, C.; Macchioni, A.; Bochmann, M. *Organometallics* **2005**, *24*, 1315.
(64) Vroegop, C. T.; Teuben, J. H.; van Bolhuis, F.; van der Linden, J. G. M. *J. Chem. Soc., Chem. Commun.* **1983**, 550.
(65) Cabrera, L.; Hollink, E.; Stewart, J. C.; Wei, P.; Stephan, D. W. *Organometallics* **2005**, *24*, 1091.
(66) Allen, F. H.; Kennard, O. *Chem. Des. Autom. News* **1993**, *8*, 1&31.
(67) The United Kingdom Chemical Database Service. Fletcher, D. A.; McMeeking, R. F.; Parkin, D. *J. Chem. Inf. Comput. Sci.* **1996**, *36*, 746.

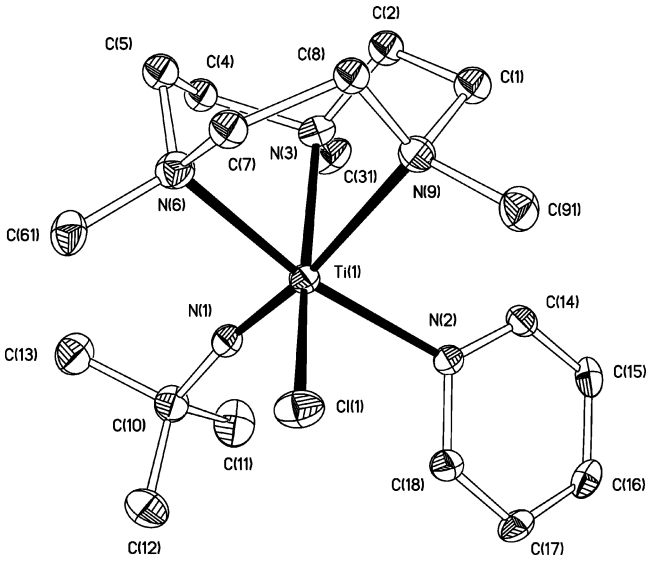

Figure 2. Displacement ellipsoid plot (25% probability) of the cation $[Ti(N^tBu)(Me_3[9]aneN_3)Cl(py)]^+$ (**9**$^+$). H atoms omitted for clarity.

Table 1. Selected Bond Lengths (Å) and Angles (deg) for $[Ti(N^tBu)(Me_3[9]aneN_3)Cl(py)]^+$ (9$^+$)

Ti(1)−N(3)	2.275(4)	Ti(1)−N(2)	2.277(3)
Ti(1)−N(6)	2.244(4)	Ti(1)−Cl(1)	2.3819(13)
Ti(1)−N(9)	2.392(3)	N(1)−C(10)	1.451(6)
Ti(1)−N(1)	1.686(4)		
Cl(1)−Ti(1)−N(3)	160.5(1)	N(6)−Ti(1)−N(1)	99.45(15)
Cl(1)−Ti(1)−N(6)	89.5(1)	N(9)−Ti(1)−N(1)	170.62(16)
N(3)−Ti(1)−N(6)	78.36(12)	Cl(1)−Ti(1)−N(2)	91.0(1)
Cl(1)−Ti(1)−N(9)	87.32(9)	N(3)−Ti(1)−N(2)	97.98(12)
N(3)−Ti(1)−N(9)	75.07(12)	N(6)−Ti(1)−N(2)	168.80(13)
N(6)−Ti(1)−N(9)	76.32(12)	N(9)−Ti(1)−N(2)	92.53(12)
Cl(1)−Ti(1)−N(1)	101.11(14)	N(1)−Ti(1)−N(2)	91.42(14)
N(3)−Ti(1)−N(1)	95.96(16)	Ti(1)−N(1)−C(10)	171.4(3)

but the exchange processes are significantly slowed at 233 K. At this temperature there are twice as many resonances observed for **10**$^+$ as would be expected for the single C_i-symmetric structure shown in Scheme 1. The ratio of the two sets of resonances is ca. 2.1:1.0, and in both cases there are resonances for bridging (δ 0.26 and 0.30 ppm, intensity 3 H) and terminal (−0.06 and 0.04 ppm, intensity 6 H) Ti−Me groups. We assign the two species as diastereomers, which differ in the relative orientations of the $Ti(N^tBu)(Me_3[9]aneN_3)Me_{terminal}$ fragments with either *trans* (as shown in Scheme 1) or *cis* arrangements of the terminal Ti−Me ligands across the Ti(μ-Me)Ti bridge. Similar features were reported recently for some methyl-bridged cyclopentadienyl-ketimide[68] and -phosphinimide[65] homobimetallic cations, and isomeric forms of methyl-bridged β-diketiminate-supported cations have also been described.[69] The compound $[Ti_2(N^tBu)_2(Me_3[9]aneN_3)_2Me_2(\mu\text{-Me})][BAr^F{}_4]$ (**10-BAr$^F_4$**) was successfully isolated in 64% yield on scale-up in C_6H_5Cl.

Cation **10**$^+$ is formally an adduct between **6**$^+$ and dimethyl **1**. A number of cationic compounds containing $\{M_2Me_2(\mu\text{-Me})\}$ units are now known.[32,63,65,68−77] The relative stability of **10**$^+$ in CD_2Cl_2 shows that the coordination of **1** to **6**$^+$ stabilizes the monomethyl cation (as mentioned, free **6**$^+$ decomposes immediately in CD_2Cl_2). However, on standing in CD_2Cl_2, resonances for **10**$^+$ slowly decrease in intensity and are replaced by a new set of signals. These are assigned to the μ-Cl-bridged cation $[Ti_2(N^tBu)_2(Me_3[9]aneN_3)_2Me_2(\mu\text{-Cl})]^+$ (**11**$^+$), which, like **10**$^+$, exists as mixture of diastereomers. This compound probably forms by dissociation of **10**$^+$ into dimethyl **1** and monomethyl cation **6**$^+$, which then immediately converts to chloride **8**$^+$. Trapping of **8**$^+$ by **1** would then (after rearrangment to put the better bridging ligand (i.e., Cl) in the bridging position) lead to **11**$^+$. Conclusive evidence for **11**$^+$ was obtained by the sequential treatment of **5** with $[Ph_3C][BAr^F{}_4]$ (1 equiv, generating **8**$^+$) and **1** (Scheme 3). The organometallic product (**11**$^+$) of this reaction sequence was identical to that arising from the slow solvent activation reaction of **10**$^+$ in CD_2Cl_2. Treatment of dimeric **11**$^+$ in CD_2Cl_2 with [PPN]Cl quantitatively re-formed **5** ($PPN^+ = [Ph_3PNPPh_3]^+$). Compound **11-BAr$^F_4$** was isolated as a yellow solid in 70% yield on the preparative scale according to Scheme 3.

Reactions of $Ti(N^tBu)(Me_3[9]aneN_3)(CH_2SiMe_3)_2$ (2) with $[PhNMe_2H][BAr^F{}_4]$ in CD_2Cl_2 and CH_2Cl_2. *N*,*N*-Dialkyl-substituted anilinium salts such as $[PhNMe_2H][BAr^F{}_4]$ are also well-established reagents for the generation of metal cations from metal-alkyl precursors (via formal protonolysis of a M−C bond).[43] However, reaction of **2** with $[PhNMe_2H][BAr^F{}_4]$ (1 equiv) in CD_2Cl_2 did not afford **7**$^+$, but instead gave ca. 50% conversion to the dichloride $Ti(N^tBu)(Me_3[9]aneN_3)Cl_2$ (**4**), together with 1 equiv of $SiMe_4$ (eq 1). The expected side-product

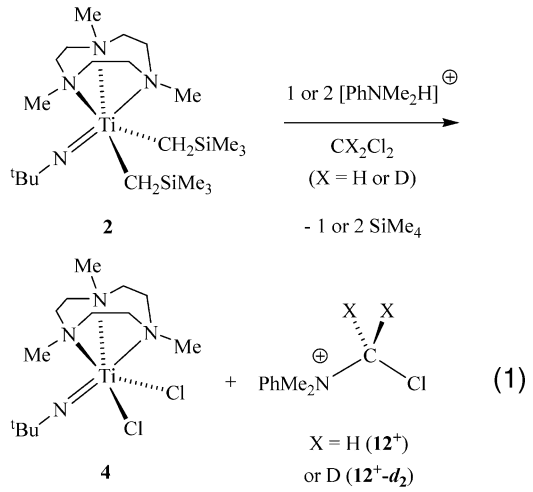

of the reaction, namely, $PhNMe_2$, was not present among the reaction products, and instead the cation $[PhNMe_2(CD_2Cl)]^+$ (**12**$^+$-***d*$_2$) was identified from the NMR spectrum and an electrospray mass spectrum (positive ion mode) of the product mixture. Reaction of **2** (eq 1) with 2 equiv of $[PhNMe_2H][BAr^F{}_4]$ on an NMR tube or preparative scale gave complete conversion to **4** together with formation of 2 equiv of either $[PhNMe_2(CD_2Cl)][BAr^F{}_4]$ (reaction in CD_2Cl_2) or $[PhNMe_2(CH_2Cl)][BAr^F{}_4]$ (**12-BAr$^F_4$**, reaction in CH_2Cl_2) and $SiMe_4$.

(68) Zhang, S.; Piers, W. E. *Organometallics* **2001**, *20*, 2088.
(69) Vollmerhaus, R.; Rahim, M.; Tomaszewski, R.; Xin, S.; Taylor, N. J.; Collins, S. *Organometallics* **2000**, *19*, 2161.
(70) Bochmann, M.; Lancaster, S. J. *Angew. Chem., Int. Ed. Engl.* **1994**, *33*, 1634.
(71) Chen, Y.; Stern, C. L.; Yang, S.; Marks, T. J. *J. Am. Chem. Soc.* **1996**, *118*, 12451.
(72) Jia, L.; Yang, Z.; Stern, C. L.; Marks, T. J. *Organometallics* **1997**, *16*, 842.
(73) Coles, M. P.; Jordan, R. F. *J. Am. Chem. Soc.* **1997**, *119*, 8125.
(74) Bochmann, M.; Green, M. L. H.; Powell, A. K.; Sassmannshausen, J.; Triller, M. U.; Wocadlo, S. *J. Chem. Soc., Dalton Trans.* **1999**, 43.
(75) Lancaster, S. J.; Bochmann, M. *J. Organomet. Chem.* **2002**, *654*, 221.
(76) Hayes, P. G.; Piers, W. E.; McDonald, R. *J. Am. Chem. Soc.* **2002**, *124*, 2132.
(77) Mehrkhodavandi, P.; Schrock, R. R.; Pryor, L. L. *Organometallics* **2003**, *22*, 4569.

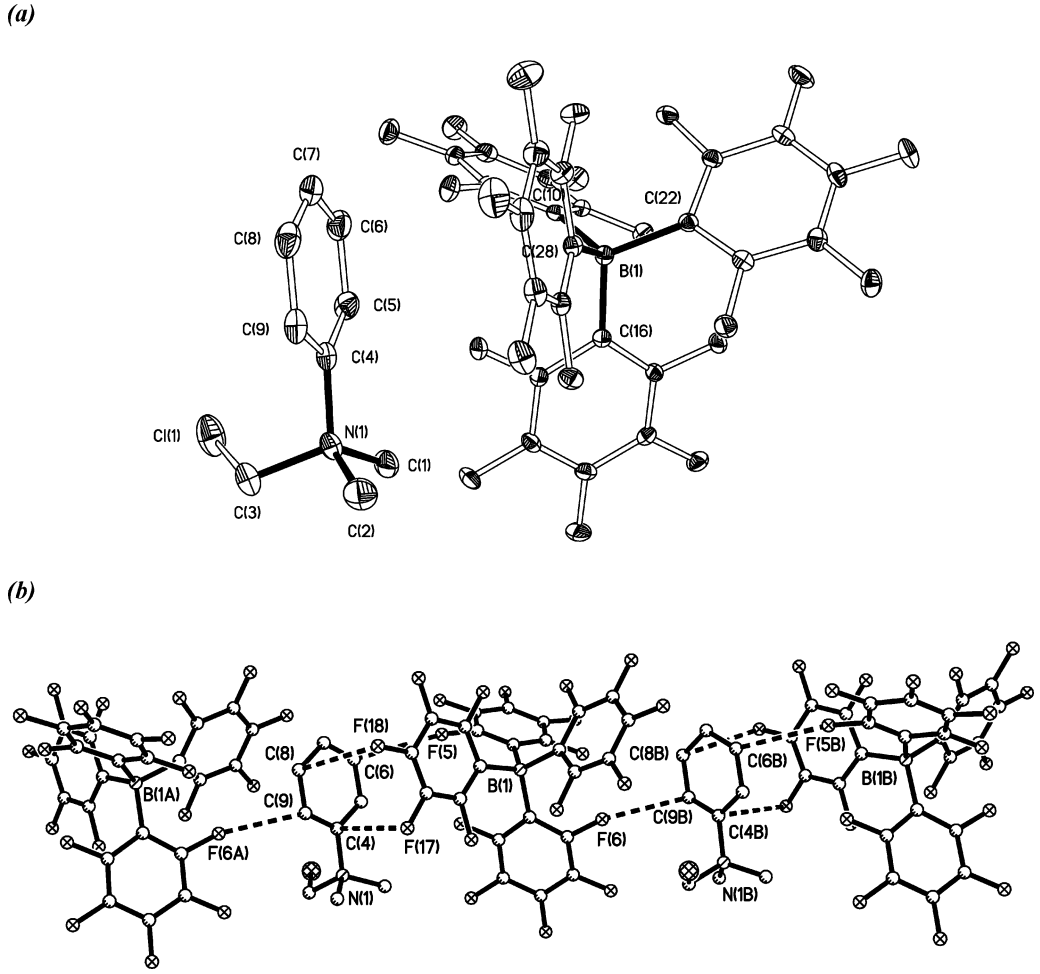

Figure 3. (a) Displacement ellipsoid plot (25% probability) of the cation−anion pair $[PhNMe_2(CH_2Cl)][BAr^F{}_4]$ (**12-BAr$^F_4$**) with H atoms omitted for clarity. (b) Intermolecular arrangements in the solid state. Atoms carrying the suffixes "A" and "B" are related to their counterparts by the symmetry operators [x, $^1/_2-y$, $z-^1/_2$] and [x, $^1/_2-y$, $z+^1/_2$] respectively.

Table 2. Selected Distances (Å) and Angles (deg) for $[PhNMe_2(CH_2Cl)][BAr^F{}_4]$ (12-BAr$^F_4$)[a]

N(1)−C(1)	1.498(4)	N(1)−C(3)	1.518(4)
N(1)−C(2)	1.516(4)	N(1)−C(4)	1.514(4)
C(1)−N(1)−C(2)	107.1(3)	C(1)−N(1)−C(3)	110.5(3)
C(2)−N(1)−C(3)	105.2(2)	C(1)−N(1)−C(4)	112.3(2)
C(2)−N(1)−C(4)	111.5(3)	C(3)−N(1)−C(4)	110.0(2)
N(1)−C(3)−Cl(1)	112.3(2)		

Closest Intermolecular C···F Distances for the $[NPhMe_2(CH_2Cl)]^+$ Cation

C(4)···F(17)	3.386(3)	C(8)···F(6A)	3.386(4)
C(6)···F(5)	3.210(4)	C(8)···F(18)	3.380(4)
C(7)···F(18)	3.394(4)	C(9)···F(6A)	2.965(3)

[a] Atoms carrying the suffixes "A" and "B" are related to their counterparts by the symmetry operators [x, $^1/_2-y$, $z-^1/_2$] and [x, $^1/_2-y$, $z+^1/_2$], respectively. Interplanar spacing between the cation phenyl ring [C(4),C(5),C(6),C(7),C(8),C(9)] and the anion ring [C(28),C(29),C(30),C(31),C(32),C(33)] = 3.49 Å.

The organic product **12-BAr$^F_4$** was isolated and the X-ray structure determined.

A view of the asymmetric unit of **12-BAr$^F_4$** is shown in Figure 3a, and selected distances and angles are listed in Table 2. The cation $\mathbf{12}^+$ has previously been structurally characterized by Choukroun as its $[BPh_4]^-$ salt (formed by reaction of Cp_2VMe_2 with $[PhNMe_2H][BPh_4]$ in CH_2Cl_2).[78] The distances and angles for $\mathbf{12}^+$ in our determination are identical to this within error. Numerous structures containing the $[BAr^F{}_4]^-$ anion have been reported.[66,67] However, unlike Choukroun's compound, crystals of **12-BAr$^F_4$** show clear evidence for supramolecular C···F interactions between the cations and anions as illustrated in Figure 3b. Each $\mathbf{12}^+$ cation interacts with two neighboring $[BAr^F{}_4]^-$ anions via a combination of offset face-to-face (interplanar spacing 3.49 Å) and edge-to-face C···F interactions. The closest intermolecular C···F distances are in the range 2.965(3)−3.394(4) Å. Supramolecular interactions between fluorinated and nonfluorinated rings are well established, and the contacts in **12-BAr$^F_4$** are within previously described ranges.[79−82] In addition to Choukroun's dichloromethane-activation reaction of Cp_2VMe_2 with $[PhNMe_2H][BPh_4]$ in CH_2Cl_2,[78] Jordan has reported that the zirconium alkyl cation $[Zr(F_6\text{-acen})(CH_2{}^tBu)(PhNEt_2)]^+$ decomposes in CH_2Cl_2 to form $[PhNEt_2(CH_2Cl)]^+$ and the chloride-bridged cation $[Zr_2(F_6\text{-acen})_2(CH_2{}^tBu)_2(\mu\text{-Cl})]^+$ (F_6-acen = $CF_3C(O)CHC(O)CF_3$).[83] Recently, Stephan has reported phosphine-based CH_2Cl_2 solvent activation mediated by transient $[CpTi(NP^tBu_3)Me(CH_2Cl_2)]^+$ to form $[(2\text{-}C_6H_4Me)_3P(CH_2Cl)][BAr^F{}_4]$

(78) Choukroun, R.; Douziech, B.; Pan, C.; Dahan, F.; Cassoux, P. *Organometallics* **1995**, *14*, 4471.

(79) Naae, D. G. *Acta Crystallogr.* **1979**, *B35*, 2765.

(80) Coates, G. W.; Dunn, A. R.; Henling, L. M.; Ziller, J. W.; Lobkovsky, E. B.; Grubbs, R. H. *J. Am. Chem. Soc.* **1998**, *120*, 3641.

(81) Vangala, V. R.; Nangia, A.; Lynch, V. M. *Chem. Commun.* **2002**, 1304.

(82) Watt, S. W.; Dai, C.; Scott, A. J.; Burke, J. M.; Viney, C.; Clegg, W.; Marder, T. B. *Angew. Chem., Int. Ed.* **2004**, *43*, 3061.

(83) Tjaden, E. B.; Swenson, D. C.; Jordan, R. F.; Petersen, J. L. *Organometallics* **1995**, *14*, 371.

Scheme 4. Mechanism for the Double-Solvent Activation Reaction of Ti(N^{t}Bu)(Me$_3$[9]aneN$_3$)(CH$_2$SiMe$_3$)$_2$ (2) on Activation with [PhNMe$_2$H][BAr$^F_4$] (2 equiv) in CH$_2$Cl$_2$[a]

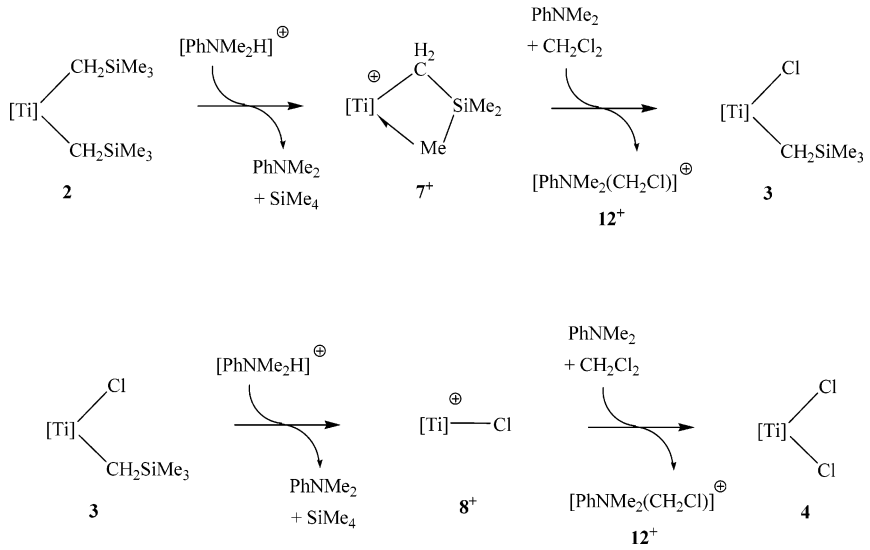

[a] Anions omitted for clarity.

and the chloride-bridged cations *rac*- and *meso*-[Cp$_2$Ti$_2$(NP^{t}Bu$_3$)$_2$Me$_2$(μ-Cl)]$^+$.[65]

A likely reaction pathway leading to **4** and **12**$^+$ is given in Scheme 4. The proposed sequence involves successive Ti−CH$_2$SiMe$_3$ bond protonolysis and solvent activation steps (via nucleophilic attack of the PhNMe$_2$ coproduct on a CH$_2$Cl$_2$ molecule activated by a highly electrophilic **7**$^+$ or **8**$^+$ cation). To account for the 50% conversion of **2** to **4** in the reaction with 1 equiv of [PhNMe$_2$H][BAr$^F_4$], it is necessary to postulate that the reaction of **3** to form **8**$^+$ is faster than that of **2** to form **7**$^+$.

Scheme 5 summarizes a series of NMR tube scale reactions carried out to test the key steps proposed in Scheme 4 for the double solvent activation reaction. Generation of **7**$^+$ in CD$_2$Cl$_2$ (using **2** and [Ph$_3$C]$^+$) followed by addition of PhNMe$_2$ gave conversion of ca. 50% of the aniline to [PhNMe$_2$(CD$_2$Cl)]$^+$ (**12**$^+$-***d*$_2$**) and a new organometallic product assigned as [Ti$_2$(N^{t}Bu)$_2$(Me$_3$[9]aneN$_3$)$_2$(CH$_2$SiMe$_3$)$_2$(μ-Cl)]$^+$ (**13**$^+$). The cation **13**$^+$ is related to Jordan's [Zr$_2$(F$_6$-acen)$_2$(CH$_2$^{t}Bu)$_2$(μ-Cl)]$^+$ and is the direct analogue of the fully characterized μ-Cl-bridged methyl titanium species **11**$^+$ (Scheme 3). Cation **13**$^+$ reacts only very slowly with the remaining PhNMe$_2$. Its formation presumably involves nucleophilic attack by PhNMe$_2$ on the CD$_2$Cl$_2$ solvent (promoted by **7**$^+$) to form the monoalkyl-monochloride product Ti(N^{t}Bu)(Me$_3$[9]aneN$_3$)Cl(CH$_2$SiMe$_3$) (**3**) as proposed in Scheme 4. However, it appears that when **3** is formed in the presence of a large excess of unreacted and highly Lewis acidic **7**$^+$, it is trapped as the μ-Cl-bridged cation **13**$^+$. In agreement with this hypothesis we found (Scheme 5) that addition of preformed **3** to alkyl cation **7**$^+$ quantitatively formed **13**$^+$. The cationic dimer itself can be cleaved by addition of [PPN]Cl to form **3**. Cation **7**$^+$ is therefore competent for CD$_2$Cl$_2$ solvent activation with PhNMe$_2$, validating the first part of the sequence proposed in Scheme 4. We also found that reaction of **3** with [PhNMe$_2$H]$^+$ in CD$_2$Cl$_2$ cleanly formed **4** (Scheme 5) in accordance with the final part of the sequence proposed in Scheme 4. Reaction of preformed choride cation **8**$^+$ with PhNMe$_2$ in CD$_2$Cl$_2$ also led to the formation of **12**$^+$-***d*$_2$** and **4**, showing that both the alkyl cation **7**$^+$ and the chloride cation **8**$^+$ are capable of promoting the solvent activation reaction.

It is interesting to note that addition of PhNMe$_2$ to [Ti(N^{t}Bu)(Me$_3$[9]aneN$_3$)X]$^+$ (X = CH$_2$SiMe$_3$ (**7**$^+$) or Cl (**8**$^+$)) leads to immediate CH$_2$Cl$_2$ activation, while no corresponding solvent activation reaction occurs with pyridine (see Scheme 3 and below). Indeed, the adduct formed with **8**$^+$ (i.e., **9**$^+$) appears to be indefinitely stable in CH$_2$Cl$_2$ or CD$_2$Cl$_2$. The different behavior of the two amines may be explained in terms of their relative nucleophilicities and Lewis basicities as previously discussed by Jordan for the different reactivities of [Zr(F$_6$-acen)(CH$_2$^{t}Bu)]$^+$ with the amines NEt$_3$, NEt$_2$Ph, NMe$_2$Ph, and NMePh$_2$.[83]

Reactions of Monoalkyl Cations [Ti(N^{t}Bu)(Me$_3$[9]aneN$_3$)R]$^+$ (R = Me (6$^+$) or CH$_2$SiMe$_3$ (7$^+$)) with Lewis Bases. Reactions of the in situ-generated monoalkyl cations **6**$^+$ and **7**$^+$ with Ph$_3$PO and pyridine are summarized in Scheme 6. The reactions with Ph$_3$PO formed the simple adducts [Ti(N^{t}Bu)(Me$_3$[9]aneN$_3$)R(Ph$_3$PO)]$^+$ (R = Me (**14**$^+$) or CH$_2$SiMe$_3$ (**15**$^+$)) in ca. 70−80% isolated yield. These fully characterized products gave the expected C_1-symmetric NMR spectra. The ^{29}Si NMR shift of −0.7 ppm (CD$_2$Cl$_2$) for **15**$^+$ is in the normal range, confirming that the high-field-shifted value of −15.9 ppm in **7**$^+$ is not simply an inductive or similar effect of the overall positive charge on this cation. Surprisingly, attempts to form corresponding adducts with THF or PMe$_3$ were unsuccessful, giving ill-defined mixtures.

Reaction of cation **6**$^+$ with pyridine at low temperature gave the anticipated adduct [Ti(N^{t}Bu)(Me$_3$[9]aneN$_3$)Me(py)]$^+$ (**16**$^+$) in 52% isolated yield. Compound **16-BAr$^F_4$** has been fully characterized, and its NMR spectra are consistent with a C_1-symmetric cation. Although **16**$^+$ is reasonably stable in the solid state, a new species was cleanly formed after 2 days in solution at room temperature. This was identified as the cation [Ti(N^{t}Bu)(Me$_3$[9]aneN$_3$)(NC$_5$H$_4$)]$^+$ (**17**$^+$, Scheme 6), containing an *ortho*-metalated pyridine ligand. The NMR tube scale reaction of **7**$^+$ with pyridine showed immediate conversion to **17**$^+$ with no observation of the expected pyridine adduct [Ti(N^{t}Bu)(Me$_3$[9]aneN$_3$)(CH$_2$SiMe$_3$)(py)]$^+$. Compound **17-BAr$^F_4$** was obtained on a preparative scale from the reaction of pyridine with in situ-generated **7-BAr$^F_4$**. Although it was not possible to obtain an analytically pure sample, the spectroscopic data were fully consistent with the structure proposed in Scheme 6.

The room-temperature ^{1}H NMR spectrum of **17**$^+$ featured broad resonances in the macrocycle region (3.20−2.50 ppm). Cooling of the sample to 203 K failed to give a "frozen out"

Scheme 5. Reactions Associated with the Ti(N^{t}Bu)(Me$_3$[9]aneN$_3$)(CH$_2$SiMe$_3$)$_2$/[PhNMe$_2$H][BAr$^F_4$] Solvent Activation System[a]

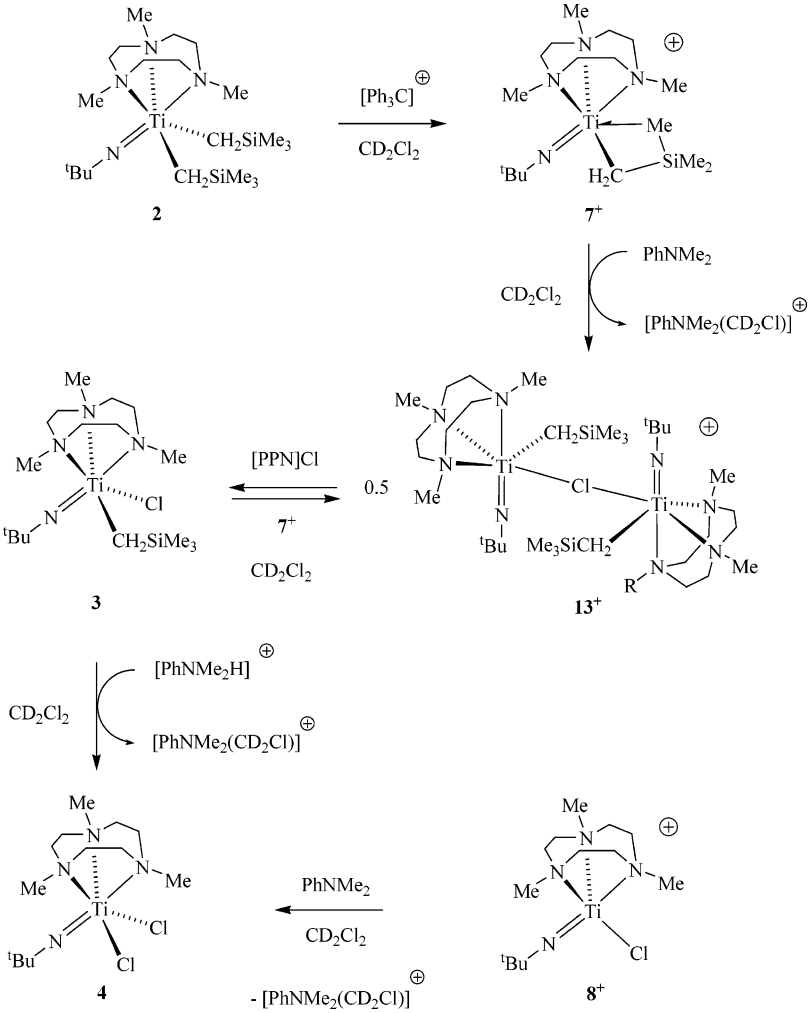

[a] Anions omitted for clarity.

Scheme 6. Reactions of [Ti(N^{t}Bu)(Me$_3$[9]aneN$_3$)R]$^+$ (R = Me or CH$_2$SiMe$_3$) with Ph$_3$PO and Pyridine[a]

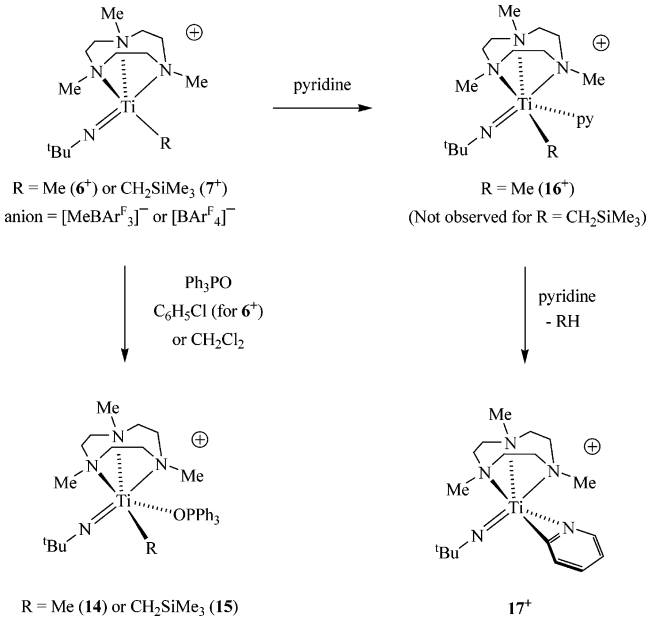

[a] Anions omitted for clarity.

spectrum, so spectra were recorded for convenience at 313 K in the fast exchange limit. At this temperature the macrocycle gives rise to two multiplets at 3.07 and 2.94 ppm, corresponding to methylene protons "up" and "down" with respect to the metal center, and a broad singlet at 2.60 ppm corresponding to the N-methyl groups. This is reminiscent of the five-coordinate methyl cation **6**$^+$. Four sharp multiplets at 8.50, 7.97, 7.75, and 7.35 ppm, each of integral 1 H, correspond to the NC_5H_4 ligand. These multiplets showed the expected couplings in a ^{1}H−^{1}H COSY spectrum and, along with the ^{13}C resonances, are in excellent agreement with those of the metalated pyridine in $[Cp_2Zr(NC_5H_4)(L)]^+$ (L = py or THF) reported by Jordan.[84] On the basis of this literature precedent and the pronounced Lewis acidity of the 14 valence electron cations [Ti(N^{t}Bu)(Me$_3$[9]aneN$_3$)X]$^+$, we favor the 16 valence electron η^2-bound isomer as illustrated (Scheme 6). However, the highly fluxional nature of this cation indicates that the interaction between the pyridyl nitrogen and the metal center may be rather weak.

The NMR tube scale reaction of **7**$^+$ with pyridine-d_5 in CH_2Cl_2 formed [Ti(N^{t}Bu)(Me$_3$[9]aneN$_3$)(NC$_5$D$_4$)]$^+$ (**17**$^+$-***d*$_4$**) as the organometallic product. The ^{2}H NMR spectrum of the product mixture featured resonances for an *ortho*-metalated 2-NC_5D_4 ligand of **17**$^+$-***d*$_4$**, together with an additional resonance at 0.0 ppm (integrating as 1 D with respect to the 2-NC_5D_4 ligand), which is attributed to the expected side-product $SiMe_4$-d_1.

(84) Jordan, R. F.; Taylor, D. F.; Baenziger, N. C. *Organometallics* **1990**, *9*, 1546.

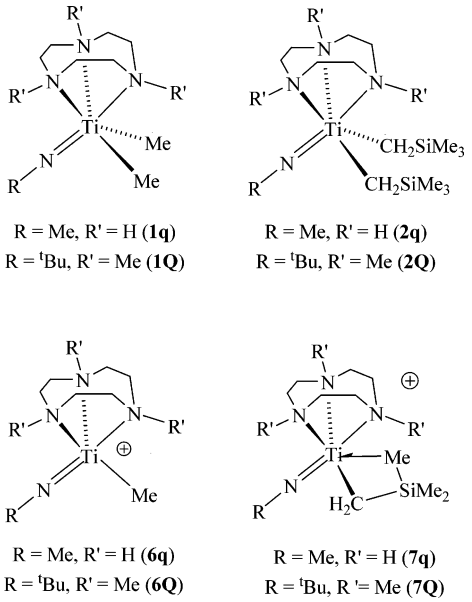

Figure 4. Model triazacyclononane-imido titanium dialkyl and monoalkyl systems studied by DFT.

The *ortho*-metalation of pyridine in this way is reminiscent of the reaction of the zirconocene methyl cation $[Cp_2ZrMe(THF)]^+$ with this ligand,[84] but contrasts with reports that the cationic titanocene $[Cp_2TiMe(py)][BPh_4]$[85] and cyclopentadienyl-phosphinimide species $[CpTi(NP^tBu_3)Me(L)]^+$ (L = py, 4-NC_5H_4Et, 4-$NC_5H_4{}^tBu$, 4-$NC_5H_4NMe_2$)[65] are stable in this regard. We note also that the related neutral compound $Cp^*Ti(N^tBu)(CH_2SiMe_3)(py)$ does not undergo *ortho*-metalation of the pyridine ligand, and neither does the 14 valence electron benzamidinate species $Ti(N^tBu)\{PhC(NSiMe_3)_2\}(CH_2SiMe_3)(py)$.[86]

DFT Studies. The remainder of this contribution focuses mainly on the electronic and molecular structures and NMR properties of the monoalkyl cations $[Ti(N^tBu)(Me_3[9]aneN_3)Me]^+$ (**6**$^+$) and $[Ti(N^tBu)(Me_3[9]aneN_3)(CH_2SiMe_3)]^+$ (**7**$^+$). We are also interested in comparisons with the isolobal $[Cp_2TiMe]^+$ system, for which we have measured $^1J_{CH}$ values. The model macrocycle-imido alkyl systems used are shown in Figure 4. Systems with labels carrying the suffix "**Q**" correspond exactly to the experimental species (Scheme 1) modeled in full, whereas those with the labels "**q**" have the macrocycle and imido N-substituents Me and *tert*-butyl replaced by H and Me, respectively. The systems "**q**" allow us to probe the underlying electronic factors, while the computationally more expensive systems "**Q**" include the full steric and electronic influences of the N-donor ligands. We begin with a comparison of the frontier orbitals of $[Cp_2Ti]^{2+}$ and $[Ti(NR)(R_3[9]aneN_3)]^{2+}$ and the basic structural preferences of the monocationic model hydrido complexes $[Cp_2TiH]^+$ and $[Ti(NMe)(H_3[9]aneN_3)H]^+$. The structure and bonding of metallocene compounds of the type $[Cp_2MX]^{n+}$ (n = 0, 1; X = none, H, methyl) have been extensively studied by a number of computational methods including extended Hückel theory (EHT), restricted Hartree−Fock (RHF), generalized valence bond (GVB), and density functional theory (DFT), sometimes with contradictory results.[54−56,87−95] The purpose of our studies was not to re-evaluate or reinvestigate previous computational work on titanocenium systems, but instead to compare the metallocene and imido-macrocyclic systems using an identical methodology (DFT (B3PW91)) and basis sets, and to use these results to aid interpretation of the available experimental observables.

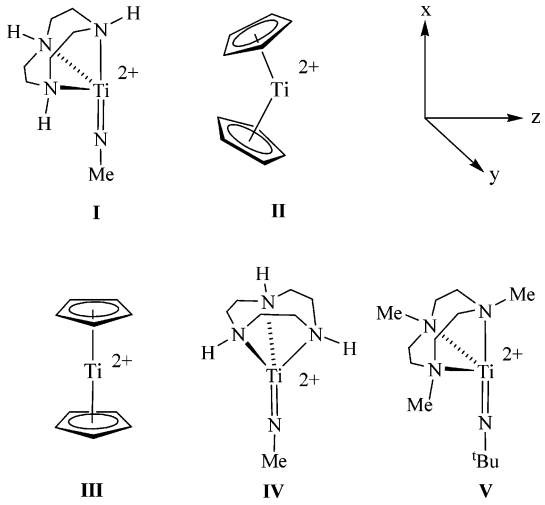

Figure 5. Model dicationic model systems compared using DFT with the chosen coordinate system.

Comparison of the Isolobal Fragments $[Cp_2Ti]^{2+}$ and $[Ti(NMe)(H_3[9]aneN_3)]^{2+}$. The ligands *fac*-$R_3[9]aneN_3$ (R = H or hydrocarbyl), η^5-$C_5R_5^-$, and RN^{2-} formally donate six electrons to a metal center through one σ and two π type interactions. Therefore, as anticipated in Figure 1, the dicationic macrocycle-imido fragment $[Ti(NR)(R_3[9]aneN_3)]^{2+}$ should be isolobal with $[Cp_2Ti]^{2+}$. However, the spatial details and energies of the frontier orbitals of these two fragments may be expected to differ in certain ways (for example, the all-carbon donor C_5R_5 ligands also have δ acceptor properties, whereas the N-coordinated $R_3[9]aneN_3$ and RN possess only donor characteristics). We therefore start our discussion with a comparison of the two model fragments $[Ti(NMe)(H_3[9]aneN_3)]^{2+}$ (**I**) and $[Cp_2Ti]^{2+}$ (**II**), as illustrated in Figure 5.

In their seminal paper,[88] Lauher and Hoffmann used EHT calculations to describe the frontier orbitals of bis(cyclopentadienyl) complexes Cp_2ML_n. For d^0 metals it was shown that a C_{2v} bent geometry for the Cp_2M fragment was preferred over the analogous D_{5h} structure with coplanar η-C_5H_5 rings. The three lowest unoccupied molecular orbitals (MOs, illustrated in Figure 6) are ideally suited to bind one or more ligands L in the equatorial (yz) plane. For the purposes of comparison with the frontier MOs of **I** (vide infra), DFT (B3PW91) calculations were carried out on $[Cp_2Ti]^{2+}$ (**II**). These yielded results analogous to those found with EHT, with a minimized C_{2v} bent structure (ring centroid−Ti−centroid angle = 138.6°) being 85.1 kJ mol^{-1} more stable than the corresponding D_{5h} one with coplanar C_5H_5 rings, i.e., **III**. The shapes and energies of the

(85) Bochmann, M.; Wilson, L. M.; Hursthouse, M. B.; Short, R. L. *Organometallics* **1987**, *6*, 2556.
(86) Stewart, P. J.; Blake, A. J.; Mountford, P. *Organometallics* **1998**, *17*, 3271.
(87) Green, J. C. *Chem. Soc. Rev.* **1998**, *27*, 263.
(88) Lauher, J. W.; Hoffmann, R. *J. Am. Chem. Soc.* **1976**, *98*, 1729.
(89) Kawamura-Kuribayasbi, H.; Koga, N.; Morokuma, K. *J. Am. Chem. Soc.* **1992**, *114*, 8687.
(90) Ziegler, T.; Folga, E.; Berces, A. *J. Am. Chem. Soc.* **1993**, *115*, 636.
(91) Bierwagen, E. P.; Bercaw, J. E.; Goddard, W. A. *J. Am. Chem. Soc.* **1994**, *116*, 1481.
(92) Woo, T. K.; Fan, L.; Ziegler, T. *Organometallics* **1994**, *13*, 2252.
(93) Fan, L.; Harrison, D.; Woo, T. K.; Ziegler, T. *Organometallics* **1995**, *14*, 2018.
(94) Yoshida, T.; Koga, N.; Morokuma, K. *Organometallics* **1995**, *14*, 746.
(95) Green, J. C.; Jardine, C. N. *J. Chem. Soc., Dalton Trans.* **2001**, 274.

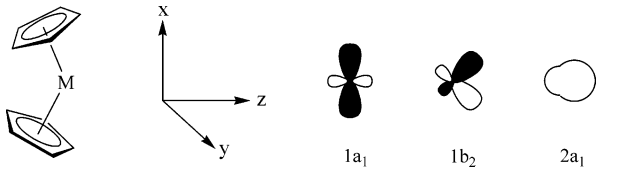

Figure 6. C_{2v}-symmetric Cp_2M unit, the chosen coordinate system, and the three lowest unoccupied molecular orbitals that lie in the *yz* molecular plane.[88]

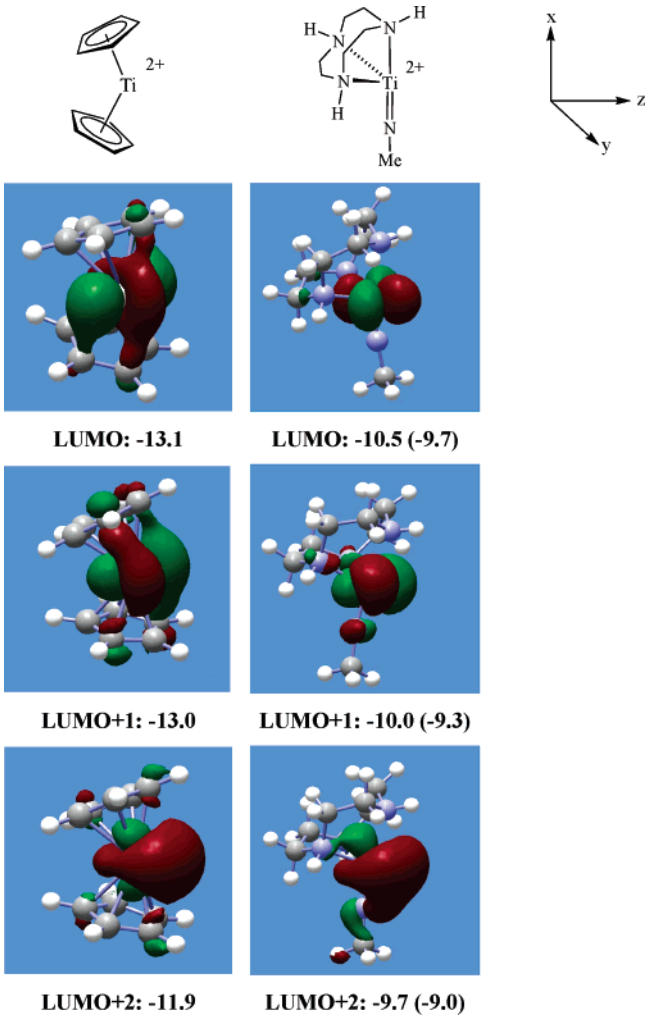

Figure 7. Three lowest unoccupied MOs for $[Cp_2Ti]^{2+}$ (**II**, left) and $[Ti(NMe)(H_3[9]aneN_3)]^{2+}$ (**I**, right), their corresponding energies (eV), and the chosen coordinate system. Values for $[Ti(N^tBu)(Me_3[9]aneN_3)]^{2+}$ (**V**) are given in parentheses.

three lowest unoccupied molecular orbitals of **II** (Figure 7) are very similar to those obtained at the EHT level and consist essentially of $3d_{y^2}$ ($1a_1$), $3d_{yz}$ ($1b_2$), and $3d_{x^2-z^2}$ ($2a_1$) orbital character in the coordinate system chosen.

The optimized geometry of $[Ti(NMe)(H_3[9]aneN_3)]^{2+}$ is the C_s-symmetric structure **I** illustrated in Figure 5 and is best described as an octahedron lacking two *cis* ligands in the *yz* plane. However, it can also be compared to that of a "bent metallocene" if the $H_3[9]aneN_3$ and NMe ligands are taken to formally replace two Cp rings. In this sense it is interesting to compare the N_3 ligand centroid−Ti−N_{imide} angle of 142.7° in **I** with the computed ring centroid−Ti−centroid angle of 138.6° in minimized **II**. The C_3-symmetric isomer of $[Ti(NMe)(H_3[9]aneN_3)]^{2+}$ (illustrated as **IV** in Figure 5) is the isolobal analogue of the D_{5h} isomer of $[Cp_2Ti]^{2+}$ (**III**). The DFT-calculated structure **IV** (minimized with the N_3 ring centroid−Ti−N_{imide} angle constrained to be 180°) was found to be less stable than the ground-state structure **I**, but only by 19.7 kJ mol^{-1}. The fragment **I**, bearing π-donor ligands, is therefore easier to distort from its ground-state geometry than the classical metallocene **II**, as already observed by Ziegler on smaller model systems.[96] It is likely that the inclusion of sterically demanding R-groups in $[Ti(NR)(R_3[9]aneN_3)]^{2+}$ would destabilize the C_s type structure **I** relative to a C_3-symmetric alternative of the type **IV**.

The shapes of three lowest unoccupied molecular orbitals of **I** (Figure 7) are, at first sight, generally analogous to those of the isolobal metallocenium system **II** (as anticipated from the isolobal analogy). The LUMO of **I** is predominantly a nonbonding $3d_{z^2-y^2}$ orbital (see Figure 7 for the definition of the coordinate system) formally originating from the t_{2g} orbital set of a σ-only bonded octahedron. The two other members of this t_{2g} set ($3d_{xz}$ and $3d_{xy}$) are pushed up in energy as a result of strong π-donation from the imido ligand. The LUMO+1 in Figure 7 (mainly $3d_{yz}$) is derived from the e_g set of this former octahedron and stabilized by the formal removal of the two *cis* ligands. The orbitals of the *cis*-divacant octahedral fragment ML_4 have been described previously.[97] DFT calculations were also carried out on the fully N-substituted system $[Ti(N^tBu)(Me_3[9]aneN_3)]^{2+}$ (**V**). The shapes of the frontier orbitals of **V** are the same as those of **I**, but the incorporation of the electron-releasing N-alkyl groups clearly leads to a destabilization of the three frontier orbitals by some 0.7−0.8 eV.

Although the three frontier MOs of $[Ti(NMe)(H_3[9]aneN_3)]^{2+}$ (**I**) and $[Cp_2Ti]^{2+}$ (**II**) are broadly similar, there are some important key differences. First, the MOs of **II** lie globally at significantly lower energies than those of **I** or **V**, making the latter two fragments much less electrophilic than **II**. A second key difference concerns the shapes of the LUMOs and their energies relative to the LUMO+1 and LUMO+2 levels. For **II** the LUMO lies close in energy to the LUMO+1 (difference ca. 0.1 eV) but some 1.2 eV below LUMO+2. In **I** and **V** there is a more sizable gap between the LUMO and LUMO+1 (0.5−0.6 eV) but a somewhat smaller one between LUMO and LUMO+2 (0.7−0.8 eV). Furthermore, the LUMO in **I** and **V** is spatially rather well oriented to form a σ bond with a donor ligand approaching along the molecular *z* axis, whereas that of **II** is rather poor in this regard, as discussed previously.[88] In fact, a better σ overlap is achieved with LUMO+2, the highest energy of the three frontier orbitals of a d^0 Cp_2M fragment.[88] As a consequence of the particular shapes and energies of the frontier orbitals, Lauher and Hoffmann predicted (using EHT) that the model σ donor hydride ligand in hypothetical $[Cp_2TiH]^+$ (**VI**) would not lie on the molecular C_2 rotation axis, but would move off this axis by an angle (α) of ca. 65° and hence achieve an optimum overlap/interaction with all three frontier orbitals of the metallocene unit. Ab initio (GVB) calculations have confirmed this result for **VI**.[91] In general, previous calculations for model group 4 metallocenium cations $[Cp_2MX]^+$ (X = H, Me)[89,91,92,94] and cationic constrained geometry analogues $[(\eta^5,\eta^1\text{-}C_5H_4SiH_2NH)M\text{-}Me]^+$ (M = Ti, Zr)[93] have found either a clear bias toward analogous distorted geometries or that the potential surface toward such a distorted geometry is rather flat.

As a simple probe of the geometric preferences of a five-coordinate system $[Ti(NR)(R'_3[9]aneN_3)X]^+$ (reference points for studies of the real systems $[Ti(N^tBu)(Me_3[9]aneN_3)Me]^+$ (**6**$^+$) and $[Ti(N^tBu)(Me_3[9]aneN_3)(CH_2SiMe_3)]^+$ (**7**$^+$)), we car-

(96) Margl, P.; Deng, L.; Ziegler, T. *Top. Catal.* **1999**, *7*, 187.
(97) Albright, T. A.; Burdett, J. K.; Whangbo, M.-H. *Orbital Interactions in Chemistry*; Wiley-Interscience: New York, 1985.

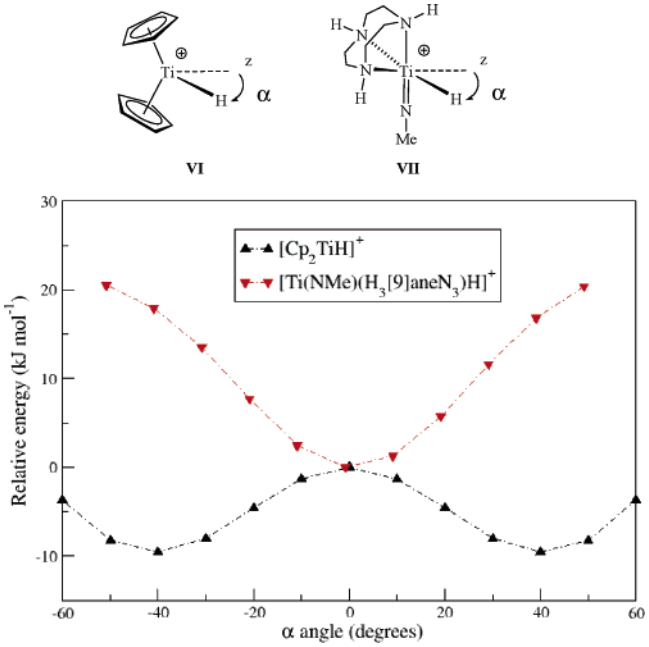

Figure 8. Variation of the relative energies of $[Cp_2TiH]^+$ (**VI**) and $[Ti(NMe)(H_3[9]aneN_3)H]^+$ (**VII**) as the angle α is varied from −50° to +50°.

ried out a series of calculations on the model hydride cation $[Ti(NMe)(H_3[9]aneN_3)H]^+$ (**VII**), in which the angle α was varied from −50° to +50° (see Figure 8). For the purposes of comparison using the same methodology and basis functions, analogous calculations were performed with DFT for $[Cp_2TiH]^+$ (**VI**). For **VI** a minimum was found for α = 42°, which compares favorably with the value of 65° found by EHT. The geometry with α = 42° lies 9.6 kJ mol^{-1} below that with α = 0° (which in fact corresponds to a transition state). In contrast, the isolobal cation **VII** is most stable when α = 0° (i.e., a nondistorted trigonal bipyramid), while at α = 42° it has an energy some 18 kJ mol^{-1} above that for α = 0°. The stability of **VII** to distortion is attributed to the more favorable shape of the LUMO for *σ* bonding in the *z* axis direction and the larger energy between LUMO and the LUMO+1 (note again that the frontier orbitals of **I** already lie ca. 2.5 eV above those of **II**).

Neutral Titanium Alkyl Compounds. The neutral macrocycle-imido dialkyl systems (see Figure 4) and Cp_2TiMe_2 were computed as reference points for the changes induced by the cationic nature of the monoalkyls and also to test the accuracy of our computational strategy since the X-ray structures for both **1** and Cp_2TiMe_2 are available.[28,98] Details of the optimized geometries are given in Figures S1 (Cp_2TiMe_2, **1q**, **1Q**) and S2 (**2q**, **2Q**) and Tables S1 (Cp_2TiMe_2, **1q**, **1Q**) and S2 (**2q**, **2Q**) of the Supporting Information. The agreement between the experimental and the calculated structures is very good for the simple model **1q**, whereas **1Q** presents some deviations for the least strongly bound ligand, $Me_3[9]aneN_3$, which is pushed further away from the metal center in **1Q** than in the experimental system **1**. This may be due to the steric repulsions between the bulky ligands ($Me_3[9]aneN_3$ and N^{t}Bu) in **1Q** not being compensated for by crystal-packing forces as in the X-ray structure. However, the bonding situation for the imido ligand is better reproduced in **1Q** than in **1q**, with an N−C bond distance (**1**, 1.438(3) Å; **1q**, 1.423 Å; **1Q**, 1.438 Å) and a Ti−N−C angle (**1**, 171.5(2)°; **1q**, 175.8°; **1Q**, 170.1°) in excellent agreement with the experimental data. Moreover, the

(98) Thewalt, U.; Wohrle, T. *J. Organomet. Chem.* **1994**, *464*, C17.

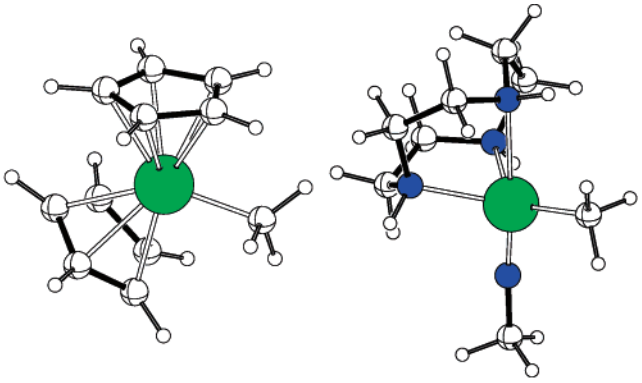

Figure 9. DFT(B3PW91)-optimized geometry for $[Cp_2TiMe]^+$ (left) and $[Ti(NMe)(H_3[9]aneN_3)Me]^+$ (**6q**, right).

agreement between experimental and calculated structures for Cp_2TiMe_2 is also excellent (Table S1), lending further credit to our computational approach.

Monomethyl Cations: Geometry and Electronic Structures. The experimental ^{29}Si NMR data for $[Ti(N^tBu)(Me_3[9]aneN_3)(CH_2SiMe_3)]^+$ (**7**$^+$) (vide supra) indicate strongly that this otherwise 14 valence electron cation possesses a *β*-Si−C···Ti agostic interaction. The nature of this interaction and other aspects associated with **7**$^+$ are addressed using DFT later on. The methyl titanium cation $[Ti(N^tBu)(Me_3[9]aneN_3)Me]^+$ (**6**$^+$) also has a formal 14 valence electron count, assuming that solvation by C_6D_5Br or interactions with $[BAr^F_4]^-$ are not significant. Hence nonclassical (in this case α-C−H agostic) interaction(s) might be expected in this species also. However, it is well-known that low valence electron counts for d^0 titanium compounds are, by themselves, no guarantee for occurrence of an α-C−H···Ti interaction (the classic examples being $TiMeCl_3$ (nonagostic[56]) and $TiMeCl_3$(dmpe) (α-agostic[99])).

We have explored the structure of **6**$^+$ and its relationship to the isolobal $[Cp_2TiMe]^+$ using DFT. As mentioned, the methyl titanocenium system $[Cp_2TiMe][MeBAr^F_3]$ has been reported to display an α-agostic interaction on the basis of vibrational spectroscopic studies.[56] Computational studies of group 4 metallocenium[89,91,92,94] and related[93,95] methyl cations have been reported before. While the extent of any α-agostic interaction predicted, and distortion of the methyl group in general, somewhat depends on the particular model system chosen and the method of calculation employed, it is generally found that the associated energies (either against or in favor) are rather small and typically no more than ca. 10−12 kJ mol^{-1}. The results we present for Cp_2TiMe^+ are not inconsistent with these previous studies.

The geometry of $[Cp_2TiMe]^+$ (Figure 9) is typical of a bent metallocene with one ligand lying in the equatorial plane. Due to the cationic nature of the complex, all bond distances to Ti are shorter than in the neutral Cp_2TiMe_2 (Table S1). At the DFT (B3PW91) level the geometry of the methyl group in $[Cp_2TiMe]^+$ clearly indicates the presence of an α-agostic interaction. One C−H bond lies in the equatorial plane and is tilted toward Ti with a significantly reduced Ti−C−H angle (83.9° vs 121.4° and 121.3° for the nonagostic C−H bonds). Moreover, the agostic C−H bond is elongated with respect to the two others (1.125 vs 1.089 and 1.080 Å). As in $[Cp_2TiH]^+$, the Ti−C_{Me} bond in $[Cp_2TiMe]^+$ no longer lies on the molecular *z* axis (see above definition), but the departure from the

(99) Dawoodi, Z.; Green, M. L. H.; Mtetwa, V. S. B.; Prout, K.; Schultz, A. J.; Williams, J. M.; Koetzle, T. F. *J. Chem. Soc., Dalton Trans.* **1986**, 1629.

symmetric structure as measured by the α angle is less pronounced than in $[Cp_2TiH]^+$ ($[Cp_2TiMe]^+$, α = 18°; $[Cp_2TiH]^+$, α = 42°).[91]

In d^0 methyl complexes, the driving force for any deformation is the increase of the number of *n*d orbitals used to make bonds to the methyl group.[55,56,100] Upon tilting, some occupied orbitals of CH_3 may interact with the low-lying empty orbitals, essentially of d character, of the metallic fragment. Such a mixing is efficient only where an empty MO of appropriate symmetry is close in energy to the occupied MO centered on CH_3. This tilting will be favored only when mixing among the empty orbitals allows for the main bonding Ti−C interaction to be preserved. In α-agostic $[Cp_2TiMe]^+$, the main bonding interaction for a sp^3 lone pair of CH_3 is with the $1b_2$ orbital of $[Cp_2Ti]^{2+}$ (**II**) and leads to the computed distorted geometry (α ≠ 0). The small energy difference between the $1a_1$ and $1b_2$ MOs of **II** allows efficient mixing between them to maintain efficient overlap with the CH_3 lone pair upon tilting. It also leaves the $1b_2$ MO more available to accept electron density from the σ(C−H) bond of CH_3 in the equatorial plane, as previously discussed by Eisenstein and Jean.[100] This bonding pattern is best illustrated by the participation of the CH_3 sp^3 lone pair and σ(C−H) bond in the LUMO and LUMO+1 of Cp_2TiMe^+ (Figure S3 in the Supporting Information). It appears that it is the requirement for both the sp^3 lobe of CH_3 and the in-plane α-agostic C−H to interact with the relevant frontier MOs of **II** that provides for a smaller deformation angle α in $[Cp_2TiMe]^+$ (α = 18°) than in $[Cp_2TiH]^+$ (α = 42°), which needs only consider the overlap of the isotropic H 1s orbital.

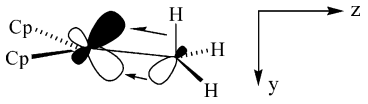

The deformation of the methyl group in $[Ti(NMe)(H_3[9]aneN_3)Me]^+$ (**6q**, Figure 9) is much less pronounced than in $[Cp_2TiMe]^+$. Nonetheless, one C−H bond lies in the equatorial plane and is tilted toward Ti with a smaller Ti−C−H angle than the two other bonds (105.9° vs 115.7° and 113.8°). However, there is no substantial lengthening of that bond (1.105 Å) with respect to the other values (1.100 and 1.094 Å). The difference between **6q** and $[Cp_2TiMe]^+$ can again be traced to the differences in shape and energies of the frontier orbitals of $[Ti(NMe)(H_3[9]aneN_3)]^{2+}$ (**I**) and $[Cp_2Ti]^{2+}$ (**II**). Unlike the case for $[Cp_2TiMe]^+$, the $Ti-C_{Me}$ bond in **6q** is essentially the result of the interaction of the HOMO of CH_3^- with the LUMO of **I**, which, as described above, is well oriented for forming a σ bond along the molecular *z* axis. This orbital is already at a relatively high energy compared with those of **II** (Figure 7), and the LUMO+1 is at an even higher energy and thus is not available to provide significant extra stabilization of the CH_3 group upon tilting. Nevertheless, there are small participations of the CH_3 sp^3 lone pair and σ(C−H) bond in the LUMO and LUMO+1 of **6q** (Figure S3) that could be traced to a very weak α-agostic interaction in **6q**.

Introduction of the real groups in model **6Q** (model of the experimental system $\mathbf{6}^+$) further modifies the bonding situation. As mentioned, the three lowest unoccupied orbitals of the fragment $[Ti(N^tBu)(Me_3[9]aneN_3)]^{2+}$ (**V**) are even higher in energy than those of **I** (Figure 7) as a result of the more electron-releasing nature of the ligand set. Consequently, the interaction of the C−H bond in the equatorial plane (already weak in **6q**) is not favorable, and no distortion of the Ti−Me group is observed.

(100) Eisenstein, O.; Jean, Y. *J. Am. Chem. Soc.* **1985**, *107*, 1177.

As noted above, globally the MOs of **II** lie at significantly lower energies than those of **I** or **V**, making the two latter complexes relatively much less electrophilic. It is therefore expected that electron transfer from CH_3 to the Ti center should be larger in $[Cp_2TiMe]^+$ than in **6q** and that the Ti−C bond has larger covalent character in the former than in the latter. We have computed the bond dissociation energy (BDE) for homolytic cleavage of the Ti−C bond for $[Cp_2TiMe]^+$, **6q**, and **6Q**, and the values amount to 153.1, 238.2, and 222.0 kJ mol^{-1}, respectively. This is in line with the general observation that transition metal−carbon bonds have a significant ionic component that makes an important contribution to the strength of the bond. A natural bonding orbital analysis (NBO) points to the same conclusion with the natural charges on Ti and CH_3 in agreement with a larger ionic character of Ti−C in **6q** (Ti, 1.428; CH_3, −0.426) than $[Cp_2TiMe]^+$ (Ti, 1.206; CH_3, −0.192). Finally, the weight of the hybrid on C in the σ(Ti−C) NBO is larger in **6q** (76.5%) than in $[Cp_2TiMe]^+$ (65.1%) and the percentage 2s character in the hybrid on C is also larger in **6q** (25.6%) than $[Cp_2TiMe]^+$ (22.7%). This confirms the rather different electronic demands of the Ti centers in the two isolobal complexes with a larger ionic component in the Ti−C bond of **6q**. Such a difference in effective electronegativity of the Ti-containing fragment should be reflected in different NMR parameters, as the latter are very sensitive to the actual properties of the electron density (vide infra).

To estimate the strength of the agostic interactions in $[Cp_2TiMe]^+$ and **6q**, the complexes were optimized under the geometry constraints that all valence Ti−C−H angles were fixed at a value of 109.5° and the Ti−C bond distance was kept frozen in the optimal geometry value in order not to introduce energy contributions associated with varying the Ti−C bond distances. For $[Cp_2TiMe]^+$, the constrained geometry complex was 4.9 kJ mol^{-1} less stable than the ground-state structure, whereas for **6q** the destabilization was only 1.4 kJ mol^{-1}. These energies do not reflect solely the strength of the agostic interaction, as they also contain the energy required to distort the CH_3 groups. This explains why, even though the agostic interaction is apparently stronger in $[Cp_2TiMe]^+$ (as judged by the more distorted geometry, see Figure 9), the estimated values for the strength of the agostic interaction are very close. This also illustrates the difficulty in establishing an unbiased method of evaluating the strength of any agostic interaction, for by its very nature this interaction does not involve *only* donation from a C−H bond to a transition metal center.[55,56]

Monomethyl Cations: NMR Parameters. NMR spectroscopy (including trends in $^1J_{CH}$) has been used previously to probe α-C−H···M interactions.[54,56] The experimental average $^1J_{CH}$ value of 116 Hz for the Ti−Me group in $\mathbf{6}^+$, however, shows an *increase* in magnitude from the value of 111 Hz for the dimethyl precursor **1**. The isolobal species $[Cp_2TiMe]^+$ (again assuming negligible C_6D_5Br or counterion interaction) also shows an increase in Ti−Me average $^1J_{CH}$ (rising to 129 Hz) in comparison with the neutral, nonagostic precursor Cp_2TiMe_2 ($^1J_{CH}$ = 124 Hz). Interestingly, in the same NMR solvent, Cp_2TiMe_2 and $[Cp_2TiMe]^+$ both have average Ti−Me $^1J_{CH}$ values that are ca. 13 Hz higher than their isolobal analogues **1** and $\mathbf{6}^+$, respectively.

The computed $^1J_{CH}$ coupling constants within the Ti−Me ligand for Cp_2TiMe_2, $[Cp_2TiMe]^+$, **1q**, **1Q**, **6q**, and **6Q** are listed in Table 3. The calculated average $^1J_{CH}$ value for **1q** is 5.3 Hz lower than that for **6q**, whereas the $^1J_{CH}$ value for Cp_2TiMe_2 is 2.4 Hz lower than that for $[Cp_2TiMe]^+$. Including the actual substituents on the macrocycle and imido ligands (models **1Q**

Table 3. Calculated $^1J_{CH}$ Coupling Constants for the C−H Bonds of the Methyl Ligand and 2s Character (%2s) of the Hybrid on CH_3 Used to Build the Corresponding Bond to H or Ti[a]

	1q		**6q**		Cp_2TiMe_2		$[Cp_2TiMe]^+$	
	$^1J_{CH}$	%2s	$^1J_{CH}$	%2s	$^1J_{CH}$	%2s	$^1J_{CH}$	%2s
$C-H_{eq}$	100.0	23.4	99.2	23.6	113.1	23.7	85.5	22.7
C−H	102.8	23.3	104.2	24.8	115.3	24.8	132.7	27.2
C−H	103.9	23.2	119.2	25.9	115.3	24.8	132.7	27.2
Ti−C		30.0		25.6		26.6		22.7
J_{av}	102.2		107.5		114.6		117.0	

[a] $C-H_{eq}$ stands for the C−H bond lying in the equatorial plane, and the average J_{av} value is given.

and **6Q**) did not lead to any significant difference (**1Q**, average $^1J_{CH}$ = 102.6 Hz; **6Q**, average $^1J_{CH}$ = 108 Hz). For such a very sensitive parameter as $^1J_{CH}$ these results match very well those obtained in the experimental systems. Indeed, an accuracy of ca. 10% is considered to be excellent for calculations on systems of this size,[101] and therefore the DFT results can be considered to be in nearly quantitative agreement with the experimental data.

The agostic interaction in $[Cp_2TiMe]^+$ does not induce a lowering of *average* $^1J_{CH}$ (117.0 Hz, Table 3) compared to Cp_2TiMe_2 (114.6 Hz), as might intuitively be expected. Although the coupling constant for the agostic C−H bond lying in the equatorial (*yz*) plane in the cationic complex is indeed lower (85.5 Hz) than that for the neutral complex, because the values for the two other C−H bonds are significantly larger (132.7 Hz), an overall average value of 117.0 Hz results. We will return to this point shortly.

The difference of 13 Hz in experimentally observed average $^1J_{CH}$ between Cp_2TiMe_2 and **1**, and between $[Cp_2TiMe]^+$ and $\mathbf{6}^+$, is comparable to that between $^1J_{CH}$ for CH_4 and MeCN (125 and 136 Hz, respectively).[102] For these simple organic compounds the change in $^1J_{CH}$ has been attributed to the difference in the amount of carbon 2s atomic orbital character in the C−H bonds. Thus, CN, being more electronegative than H, is associated with the increased value for $^1J_{CH}$ in MeCN because (according to Bent's rule[103]) there is less 2s orbital contribution in bonds directed to more electronegative substituents. We also note Grubbs' report that $^1J_{CH}$ values for Ti−Me groups in substituted metallocenes $(Cp^R)_2TiMeCl$ vary with the electron-donating properties of Cp^R (Cp^R = substituted cyclopentadienyl), but only over a relatively narrow range (ca. 3 Hz).[57]

An NBO analysis was performed to evaluate the amount of 2s character (%2s) in the hybrid on C used to create the Ti−C and C−H bonds in the neutral and cationic complexes shown in Table 3. The %2s value in the hybrid on CH_3 used to make the bond to Ti is lower for Cp_2TiMe_2 relative to **1q**, in agreement with a higher effective electronegativity of Ti in fragment **II** compared to **I**. Consequently, and in excellent agreement with the experimental observations, the average $^1J_{CH}$ value for the titanocene system is ca. 12 Hz larger than that for the macrocycle-imido analogue. The same reasoning explains the relative average $^1J_{CH}$ values for the cationic systems **6q** and $[Cp_2TiMe]^+$, for which there is an excellent correlation between average $^1J_{CH}$ and %2s. The overall positive charge in Cp_2TiMe^+ and **6q** increases the effective electronegativity of the L_nTi fragments for the cationic complexes and accounts, in each instance, for the larger value obtained for $^1J_{CH}$ relative to the neutral systems.

We thought it possible that the intrinsic redistribution of %2s character between the Ti−C and C−H bonds on $[Cp_2TiMe]^+$ cation formation might mask the effects of an α-agostic interaction on the average $^1J_{CH}$ *when* compared to the neutral dimethyl. As mentioned above, the model cation $[Cp_2TiMe]^+$ has also been optimized with all Ti−C−H angles fixed at a value of 109.5°. The average $^1J_{CH}$ in this species was calculated to be 121.3 Hz, ca. 4 Hz *higher* than that of the optimized agostic cation (Table 3), showing that the formation of the agostic interaction does give the expected reduction of average $^1J_{CH}$, but not in comparison with the *neutral* precursor.

Trimethylsilylmethyl Cation 7^+: Geometry and Electronic Structures. The experimental results speak in favor of the presence of a β-Si−C agostic interaction in $[Ti(N^tBu)(Me_3[9]aneN_3)CH_2SiMe_3]^+$ ($\mathbf{7}^+$), as indicated by the upfield shift of the ^{29}Si NMR resonance in comparison with the neutral dialkyl $Ti(N^tBu)(Me_3[9]aneN_3)(CH_2SiMe_3)_2$ (**2**). However, the system is highly fluxional and the proposed unsymmetric agostic structure could not be "frozen out" by NMR (Scheme 2). The optimized geometry for **2q** is shown in Figure S3 in the Supporting Information, and that of **7q** is given in Figure 10. Selected geometrical parameters are given in Table S2 in the Supporting Information. The model dialkyl complex **2q** does not possess any agostic interaction. The angles subtended at the $Ti-CH_2-Si$ methylene carbons are within the normal ranges, and the $Si_\beta-C_\gamma$ bond distances are all similar. In contrast, there is a clear β-Si−C···Ti agostic interaction in **7q** with a Ti···Si contact of 2.534 Å. The $TiCH_2SiMe_3$ group is strongly distorted, with a $Ti-CH_2-Si$ angle of 90.7° and one very elongated $Si_\beta-C_\gamma$ agostic bond (1.973 Å) for the methyl group closest to Ti. One $C_\gamma-H$ bond of this methyl group is very slightly longer than the other two (1.109 vs 1.096 and 1.095 Å), possibly as a result of an interaction with the metal center.

Two different interpretations have been offered in the literature to describe β−Si−C···metal agostic interactions and, in particular, the significant lengthening of one of the $Si_\beta-C_\gamma$ bonds. Some authors consider that the elongation originates from a negative hyperconjugative donation of $\sigma(metal-C_\alpha)$ into $\sigma^*(Si_\beta-C_\gamma)$ as a result of the large ionic component of the metal−C bond.[55,56,60] Others consider that the main driving force is donation from the $\sigma(Si_\beta-C_\gamma)$ bond into an empty valence orbital on the metal, following the classical description of agostic interactions.[104−106] We note that although Ducéré and Cavallo have very recently used DFT to model Bochmann's cation[63] $[\{rac\text{-}Me_2Si(1\text{-}Indenyl)_2\}ZrCH_2SiMe_3]^+$ and found a β-Si−C stabilized geometry,[107] no description of the bonding was advanced.

We performed an NBO analysis of **7q** and **7Q**, and in particular examined the second-order perturbation interaction energy terms between occupied and empty NBO (Table S3 in the Supporting Information). The absolute values of these energy terms should not be considered by themselves, but the relative values are indicative of the importance of the various contributions. There is not a single strong contribution and many terms are involved in the agostic interaction. The hyperconjugative donation is the weakest, as bonding to d-block metals is less ionic than bonding to 4f-block metals, where this interaction was shown to be crucial.[108] Classical donation from both

(101) Autschbach, J. *Struct. Bond.* **2004**, *112*, 1.
(102) Maciel, G. E.; McIver, J. W.; Ostlund, N. S.; Pople, J. A. *J. Am. Chem. Soc.* **1970**, *92*, 1.
(103) Bent, H. A. *Chem. Rev.* **1961**, *61*, 275.
(104) Koga, N.; Morokuma, K. *J. Am. Chem. Soc.* **1988**, *110*, 108.
(105) Clark, D. L.; Gordon, J. C.; Hay, P. J.; Martin, R. L.; Poli, R. *Organometallics* **2002**, *21*, 5000.
(106) Brady, D. E.; Clark, D. L.; Gordon, J. C.; Hay, P. J.; Keogh, D. W.; Poli, R.; Scott, B. L.; Watkin, J. G. *Inorg. Chem.* **2003**, 6682.
(107) Ducéré, J.-M.; Cavallo, L. *Organometallics* **2006**, *25*, 1431.

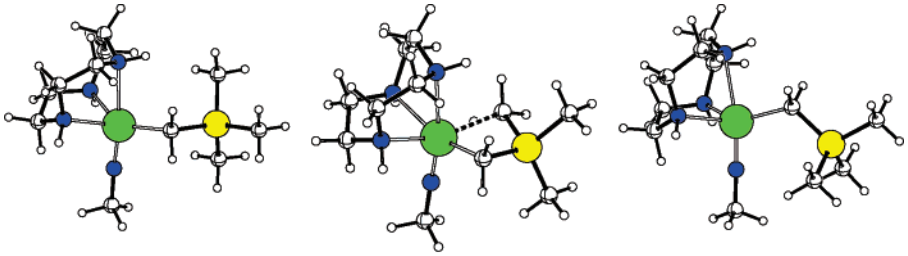

Figure 10. DFT(B3PW91)-optimized geometries and relative energies (kJ mol^{-1}) for **7q-TS1** (left), **7q** (center), and **7q-TS2** (right).

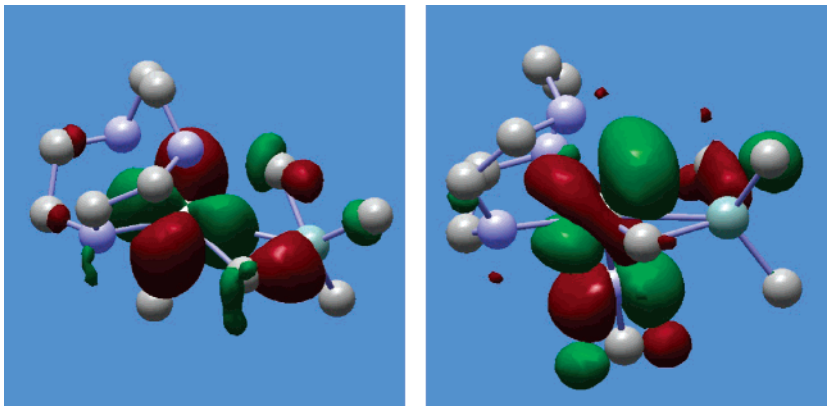

Figure 11. LUMO (left) and LUMO+1 (right) for [Ti(NMe)(H_3[9]aneN$_3$)(CH_2SiMe_3)]$^+$ (**7q**). H atoms omitted for clarity.

$Si_\beta-C_\gamma$ and $C_\gamma-H$ is an important contributor, but even more important is donation from $C_\alpha-Si_\beta$ to an empty 3d orbital on Ti. This 3d orbital is the LUMO of **I** (Figure 7), and canting the Ti−CH_2 bond away from the molecular *z* axis allows this orbital to interact with the $C_\alpha-Si_\beta$ bond. These two principal contributions are highlighted by their antibonding component clearly visible in LUMO and LUMO+1 of **7q** (Figure 11). The bonding situation for β-Si−C···metal agostic complexes is thus best described as a combination of several interactions whose respective weights depend on the precise chemical structure of the molecule under study.

The transition states involved in the fluxional process observed experimentally for **7**$^+$ were located for the smaller model **7q** and are shown in Figure 10. **7q-TS1** is the transition state associated with the exchange of the methyl groups on $SiMe_3$ between the agostic and nonagostic positions. Its energy relative to **7q** is only 14.8 kJ mol^{-1}, confirming the facile nature of the exchange process at $SiMe_3$ indicated by the solution NMR studies on **7**$^+$. The energy of this transition state could serve as an approximate estimate of the strength of the agostic interaction. However, computing the strength of an agostic interaction is not straightforward, as the definition of a suitable nonagostic reference system is not trivial. For example, in the case of **7q-TS1**, the Si−Me bond distances are not all equal, even though none is significantly elongated (Table S2). Moreover, the angle Ti−CH_2−Si slightly increases in **7q-TS1** without reaching a value similar to that in **2q**. There is thus some distortion within CH_2SiMe_3 speaking against an entirely agostic-free situation. Nevertheless, we prefer to consider that breaking the agostic interaction requires at least the exchange of the Me groups, and therefore the energy of **7q-TS1** is a lower limit of the strength of the agostic bond.

Experimentally, the two *cis* (with respect to N^{t}Bu) NMe groups on the Me_3[9]aneN$_3$ ligand of **7**$^+$ are equivalent down to low temperatures. The transition state for isomerizing the CH_2SiMe_3 chain (**7q-TS2** in Figure 10) was found at only 24.9 kJ mol^{-1} above **7q**, in agreement with an overall facile fluxional process. The energy of **7q-TS2** could serve as an upper limit for the strength of the agostic interaction, and therefore the latter could be considered to lie between 14.8 and 24.9 kJ mol^{-1}. A transition state akin to **7q-TS2** for the real system **7**$^+$ would render equivalent the two *cis* NMe groups on the Me_3[9]aneN$_3$ ligand. For the model of the real system (**7Q**) a transition-state structure similar to **7q-TS1** could not be located and only a transition state for the overall exchange (**7Q-TS2**) was found. Despite the steric congestion imposed by the N^{t}Bu and Me_3[9]aneN$_3$ ligands, the energy of this transition state is only 33.4 kJ mol^{-1} above **7Q**, in excellent agreement with the observation of equivalent *cis* Me groups for the Me_3[9]aneN$_3$ ligand of **7**$^+$, even at low temperature.

Trimethylsilylmethyl Cation 7$^+$: NMR Parameters. Calculations of the Si chemical shift for the neutral and cationic complexes yielded results in excellent agreement with the experimental data (δ −1.8 (CD_2Cl_2) or −3.1 (C_6D_5Br) ppm for **2**; δ −15.9 (CD_2Cl_2) or −17.5 (C_6D_5Br) ppm for **7**$^+$). Thus the calculated Si chemical shift in the neutral dialkyls is very close to zero (−1.2 ppm for **2q**; 0.0 ppm for **2Q**), whereas it is significantly shifted upfield in the cations (−17.6 ppm, **7q**, −20.0 ppm, **7Q**). These results lend further support for the presence of the β-Si−C agostic interaction in solution for the real cation **7**$^+$. They also show that the ^{29}Si chemical shift is a very sensitive probe to characterize the presence of an agostic interaction and may be used experimentally and computationally to characterize nonclassical bonding situations in homologous series of silicon-containing molecules.

Conclusions

We have presented a comprehensive experimental and DFT study of imido titanium alkyl cations supported by Me_3[9]aneN$_3$. The Lewis acidic nature of the readily prepared cations

(108) Perrin, L.; Maron, L.; Eisenstein, O.; Lappert, M. F. *New J. Chem.* **2003**, *27*, 121.

$[Ti(N^tBu)(Me_3[9]aneN_3)R]^+$ (**6**$^+$ and **7**$^+$) is exemplified by the formation of homobimetallic methyl- or chloride-bridged dimers, the orthometalation of pyridine, and a double solvent activation reaction when **7**$^+$ is generated using $[PhNMe_2H]^+$ in CH_2Cl_2. The presence (or not) of α-C−H or *β*-Si−C agostic interactions in $[Ti(N^tBu)(Me_3[9]aneN_3)R]^+$ has been established and interpreted by a combination of NMR and DFT techniques. A DFT comparison of the isolobal species $[Ti(NR)(R'_3[9]aneN_3)X]^{n+}$ and $[Cp_2TiX]^{n+}$ (in conjunction with NMR studies of Cp_2TiMe_2 and $[Cp_2TiMe]^+$) has highlighted and explained the key differences between them. Use of $^1J_{CH}$ coupling constants to identify α-C−H agostic interactions on the basis of differences between observed values for neutral and cationic systems may be inappropriate in cases where there are significant changes in the carbon 2s orbital contributions to the M−C and C−H bonds on cation formation.

Experimental Section

General Methods and Instrumentation. All manipulations were carried out using standard Schlenk line or drybox techniques under an atmosphere of argon or of dinitrogen. Protio- and deutero-solvents were predried over activated 4 Å molecular sieves and were refluxed over the appropriate drying agent, distilled, and stored under dinitrogen in Teflon valve ampules. NMR samples were prepared under dinitrogen in 5 mm Wilmad 507-PP tubes fitted with J. Young Teflon valves. ^{1}H, ^{13}C{^{1}H}, ^{19}F, ^{31}P{^{1}H}, ^{29}Si, and ^{2}H NMR spectra were recorded on Varian Mercury-VX 300, Varian Unity Plus 500, and Bruker AV500 spectrometers. ^{1}H and ^{13}C assignments were confirmed when necessary with the use of DEPT-135, DEPT-90, and two-dimensional ^{1}H−^{1}H and ^{13}C−^{1}H NMR experiments. ^{1}H and ^{13}C spectra were referenced internally to residual protio-solvent (^{1}H) or solvent (^{13}C) resonances and are reported relative to tetramethylsilane ($\delta = 0$ ppm). ^{19}F, ^{31}P{^{1}H}, and ^{29}Si spectra were referenced externally to $CFCl_3$, 85% H_3PO_4, and tetramethylsilane, respectively. Chemical shifts are quoted in δ (ppm) and coupling constants in Hertz. Infrared spectra were prepared as Nujol mulls between NaCl plates and were recorded on Perkin-Elmer 1600 and 1710 series FTIR spectrometers. Infrared data are quoted in wavenumbers (cm^{-1}). Mass spectra were recorded by the mass spectrometry service of Oxford University's Department of Chemistry and elemental analyses by the analytical services of the University of Oxford Inorganic Chemistry Laboratory or by the Elemental Analysis Service at the London Metropolitan University.

Literature Preparations and Other Starting Materials. The compounds $Ti(N^tBu)(Me_3[9]aneN_3)R_2$ (R = Me (**1**) or CH_2SiMe_3 (**2**)),[28] $Ti(N^tBu)(Me_3[9]aneN_3)Cl(Me)$ (**5**),[46] $Ti(N^tBu)(Me_3[9]aneN_3)Cl_2$ (**4**),[24] and Cp_2TiMe_2[109] were prepared according to published methods. The compounds $[Ph_3C][BAr^F_4]$ and $[HNMe_2Ph][BAr^F_4]$ were provided by DSM Research. All other compounds and reagents were purchased and used without further purification.

$Ti(N^tBu)(Me_3[9]aneN_3)Cl(CH_2SiMe_3)$ (3). A solution of Ph_3CCl (0.120 g, 0.43 mmol) in benzene (15 mL) was added to a stirred solution of $Ti(N^tBu)(Me_3[9]aneN_3)(CH_2SiMe_3)_2$ (**2**, 0.200 g, 0.43 mmol) in benzene (15 mL) at 5 °C in the absence of light and heated to 60 °C for 16 h. The volatiles were removed under reduced pressure, and most of the resulting yellow-brown solid was dissolved in a mixture of hexane (20 mL) and benzene (2 mL). The solution was filtered away from the remaining brown solid and cooled to −30 °C for 5 days to give **3** as yellow crystals. Yield: 0.072 g (41%). ^{1}H NMR (C_6D_6, 499.9 MHz, 293 K): 2.79 (3H, s, NMe), 2.78−2.65 (3H, overlapping m, NCH_2), 2.57 (3H, s, NMe), 2.44−2.33 (2H, overlapping m, NCH_2), 2.37 (3H, s, NMe), 2.11 (1H, m, NCH_2), 1.94 (1H, m, NCH_2), 1.89 (1H, d, ^2J 10.3 Hz, $CH_aH_bSiMe_3$), 1.71 (1H, m, NCH_2), 1.62−1.54 (2H, overlapping m, NCH_2), 1.50−1.39 (2H, overlapping m, NCH_2), 1.41 (9H, s, $NCMe_3$), 0.67 (9H, s, $SiMe_3$), −0.33 (1H, d, ^{2}J 10.3 Hz, $CH_aH_bSiMe_3$). ^{13}C{^{1}H} NMR (C_6D_6, 75.4 MHz, 293 K): 67.1 ($NCMe_3$), 56.7 (CH_2), 56.4 (CH_2), 55.8 (CH_2), 55.5 (CH_2), 54.8 (CH_2), 54.1 (CH_2), 53.2 (NMe), 52.8 (NMe), 49.3 (NMe), 43.7 (CH_2SiMe_3), 32.4 ($NCMe_3$), 4.7 ($SiMe_3$). ^{29}Si NMR (HMQC ^{1}H-observed, CD_2Cl_2, 299.9 MHz, 293 K): −1.8 (CH_2SiMe_3). IR (NaCl plates, Nujol mull, cm^{-1}): 1497 (w), 1349 (w), 1299 (w), 1242 (s), 1204 (w), 1155 (w), 1067 (m), 1011 (s), 885 (m), 851 (m), 818 (m), 781 (w), 745 (w), 681 (w), 665 (w). FIMS: *m*/*z* 414.2 (5%) $[M + H]^+$, 325.2 (67%) $[M - CH_2SiMe_3]^+$, 244.1 (100%) $[M - Me_3[9]aneN_3 + 3H]^+$, 171.2 (39%) $[Me_3[9]aneN_3]^+$, 73.0 (10%) $[^tBuNH_2]^+$. Anal. Found (calcd for $C_{17}H_{41}ClN_4SiTi$): C 49.6 (49.4), H 10.0 (10.0), N 13.7 (13.6).

NMR Tube Scale Synthesis of $[Ti(N^tBu)(Me_3[9]aneN_3)Me][BAr^F_4]$ (6-BAr^F_4). $Ti(N^tBu)(Me_3[9]aneN_3)Me_2$ (**1**, 0.008 g, 0.025 mmol) and $[Ph_3C][BAr^F_4]$ (0.023 g, 0.025 mmol) were dissolved in C_6D_5Br (0.75 mL). After 10 min a ^{1}H NMR spectrum was recorded, which showed quantitative conversion to **6-BAr^F_4** and Ph_3CMe. ^{1}H NMR (C_6D_5Br, 499.9 MHz, 293 K): 2.32 (6H, br m, CH_2), 2.17 (9H, s, NMe), 2.11 (6H, br m, CH_2), 0.89 (9H, s, $NCMe_3$), 0.65 (3H, s, $^1J_{C-H}$ 116 Hz, TiMe). ^{13}C{^{1}H} NMR (C_6D_5Br, 75.4 MHz, 293 K): 148.8 (br d, $^1J_{C-F}$ 239 Hz, 2-C_6F_5), 138.6 (br d, $^1J_{C-F}$ 251 Hz, 4-C_6F_5), 136.7 (br d, $^1J_{C-F}$ 246 Hz, 3-C_6F_5), 69.9 ($NCMe_3$), 55.0 (CH_2), 50.5 (NMe), 40.3 (TiMe), 31.4 ($NCMe_3$). ^{19}F NMR (C_6D_5Br, 282.1 MHz, 293 K): −131.8 (d, ^3J 10.6 Hz, 2-C_6F_5), −161.8 (t, ^3J 21.2 Hz, 4-C_6F_5), −165.8 (app t, app ^3J 18.1 Hz, 3-C_6F_5).

NMR Tube Scale Synthesis of $[Ti(N^tBu)(Me_3[9]aneN_3)Me][MeBAr^F_3]$ (6-$MeBAr^F_3$). $Ti(N^tBu)(Me_3[9]aneN_3)Me_2$ (**1**, 0.007 g, 0.022 mmol) and BAr^F_3 (0.011 g, 0.022 mmol) were dissolved in C_6D_5Br (0.75 mL). After 10 min a ^{1}H NMR spectrum was recorded, which showed quantitative conversion to **6-$MeBAr^F_3$**. ^{1}H NMR (C_6D_5Br, 499.9 MHz, 293 K): as above with additional peak at 1.03 (3H, br s, BMe). ^{19}F NMR (C_6D_5Br, 282.5 MHz, 293 K): −132.2 (d, ^3J 18.3 Hz, 2-C_6F_5), −163.7 (t, ^3J 16.0 Hz, 4-C_6F_5), −166.4 (app t, app ^3J 19.8 Hz, 3-C_6F_5).

NMR Tube Scale Synthesis of $[Ti(N^tBu)(Me_3[9]aneN_3)(CH_2SiMe_3)][BAr^F_4]$ (7-BAr^F_4). $Ti(N^tBu)(Me_3[9]aneN_3)(CH_2SiMe_3)_2$ (**2**, 0.010 g, 0.022 mmol) and $[Ph_3C][BAr^F_4]$ (0.020 g, 0.022 mmol) were dissolved in CD_2Cl_2 (0.75 mL). After 10 min an ^{1}H NMR spectrum was recorded, which showed quantitative conversion to **7-BAr^F_4** and "$Me_3SiCH_2BAr^F_3$". ^{1}H NMR (CD_2Cl_2, 500.0 MHz, 213 K): 3.63 (2H, m, NCH_2), 3.06 (2H, m, NCH_2), 2.95 (6H, s, NMe *cis*), 2.90−2.50 (8H, overlapping m, NCH_2), 2.40 (3H, s, NMe *trans*), 2.02 (2H, s, CH_2SiMe_3), 1.11 (9H, s, $NCMe_3$), 0.17 (9H, s, CH_2SiMe_3). ^{13}C{^{1}H} NMR (CD_2Cl_2, 125.7 MHz, 213 K): 147.6 (br d, $^1J_{C-F}$ 247 Hz, 2-C_6F_5), 137.8 (br d, $^1J_{C-F}$ 225 Hz, 4-C_6F_5), 135.9 (br d, $^1J_{C-F}$ 247 Hz, 3-C_6F_5), 69.8 ($NCMe_3$), 55.9−54.9 (series of overlapping singlets, NCH_2 and CH_2SiMe_3), 51.5 (NMe *cis*), 48.7 (NMe *trans*), 30.7 ($NCMe_3$), 1.3 ($SiMe_3$). ^{19}F NMR (CD_2Cl_2, 282.1 MHz, 293 K): −133.5 (d, ^3J 10.6 Hz, 2-C_6F_5), −164.0 (t, ^3J 20.4 Hz, 4-C_6F_5), −167.9 (app t, app ^3J 18.1 Hz, 3-C_6F_5). ^{29}Si NMR (HMQC ^{1}H-observed, CD_2Cl_2, 299.9 MHz, 293 K): −15.9 (CH_2SiMe_3). ^{29}Si NMR (HMQC ^{1}H-observed, C_5D_5Br, 299.9 MHz, 293 K): −17.5 (CH_2SiMe_3).

Synthesis of "$Me_3SiCH_2CPh_3$" from $LiCH_2SiMe_3$ and Ph_3CCl. Cold benzene (20 mL) was added to a mixture of Ph_3CCl (0.50 g, 1.79 mmol) and $LiCH_2SiMe_3$ (0.17 g, 1.79 mmol) at 5 °C with vigorous stirring. The orange suspension was allowed to warm to room temperature and then stirred for 1 h, after which it was filtered and the volatiles were removed under reduced pressure. The resulting orange oily solid was extracted into CH_2Cl_2 (20 mL) and filtered, and the volatiles were removed under reduced pressure to give an orange-yellow oil, which was distilled under reduced

(109) Erskine, G. J.; Hartgerink, J.; Weinberg, E. L.; McCowan, J. D. *J. Organomet. Chem.* **1979**, *170*, 51.

pressure (4×10^{-2} mbar, 185−195 °C). Yield: 0.30 g. Apart from a quantity (ca. 30% by ^{1}H integration) of Ph_3CH, the main components of the oil are two isomers of "$Me_3SiCH_2CPh_3$" in the ratio ca. 45 (isomer "*A*"):ca. 25 (isomer "*B*"). ^{1}H NMR (CD_2Cl_2, 299.9 MHz, 293 K): 7.37−6.85 (overlapping m, Ph), 5.57 (s, Ph_3CH), 2.12 (s, $Me_3SiCH_2CPh_3$ of isomer *A*), 2.06 (s, $Me_3SiCH_2CPh_3$ of isomer *B*), −0.01 (s, $Me_3SiCH_2CPh_3$ of isomer *B*), −0.32 (s, $Me_3SiCH_2CPh_3$ of isomer *A*). ^{13}C{^{1}H} NMR (CD_2Cl_2, 75.4 MHz, 293 K): 149.6 (1-C_6H_5), 144.3 (1-C_6H_5), 129.7 (2 or 3-C_6H_5), 129.5 (2 or 3-C_6H_5), 129.3 (2 or 3-C_6H_5, Ph_3CH), 128.7 (2 or 3-C_6H_5), 128.0 (2 or 3-C_6H_5), 127.9 (2 or 3-C_6H_5, Ph_3CH), 126.7 (4-C_6H_5), 126.1 (4-C_6H_5), 125.9 (4-C_6H_5, Ph_3CH), 57.2 (Ph_3CH), 32.0 ($Me_3SiCH_2CPh_3$ of isomer *A*), 26.6 ($Me_3SiCH_2CPh_3$ of isomer *B*), 0.3 ($Me_3SiCH_2CPh_3$ of isomer *A*), −1.9 ($Me_3SiCH_2CPh_3$ of isomer *B*). ^{29}Si NMR (HMQC ^{1}H-observed, CD_2Cl_2, 299.9 MHz, 293 K): 0.7 ($SiMe_3$ of isomer *B*), −1.1 ($SiMe_3$ of isomer *A*). GC-MS (EI): retention time 10.72 min, *m*/*z* 244 (100%) $[Ph_3C]^+$, 165 (77%) (not assigned); retention time 11.99 min, *m*/*z* 330 (5%) $[Me_3SiCH_2CPh_3]^+$, 243 (100%) $[Ph_3C]^+$, 178 (15%) (not assigned), 165 (34%) (not assigned), 135 (28%) (not assigned); retention time 12.42 min, *m*/*z* 330.1 (100%) $[Me_3SiCH_2CPh_3]^+$, 256 (20%) (not assigned), 243 (18%) $[Ph_3C]^+$, 178 (19%) (not assigned), 165 (35%) (not assigned), 73 (20%) $[SiMe_3]^+$. EI-HRMS: *m*/*z* found (calcd for $C_{23}H_{26}Si$, $[Me_3SiCH_2CPh_3]^+$) 330.1802 (330.1804).

NMR Tube Scale Synthesis of [Cp_2TiMe][BAr^F_4]. Cp_2TiMe_2 (0.0044 g, 0.021 mmol) and $[Ph_3C][BAr^F_4]$ (0.0195 g, 0.021 mmol) were dissolved in C_6D_5Br (0.75 mL). After 10 min a ^{1}H NMR spectrum was recorded, which showed quantitative conversion to the title compound and Ph_3CMe. ^{1}H NMR (C_6D_5Br, 299.9 MHz, 293 K): 5.83 (10H, s, C_5H_5), 0.96 (3H, s, $^1J_{C-H}$ 129 Hz, Me). ^{13}C{^{1}H} NMR (C_6D_5Br, 75.4 MHz, 293 K): 148.8 (br d, $^1J_{C-F}$ 239 Hz, 2-C_6F_5), 138.6 (br d, $^1J_{C-F}$ 251 Hz, 4-C_6F_5), 136.7 (br d, $^1J_{C-F}$ 246 Hz, 3-C_6F_5), 119.1 (C_5H_5), 75.6 (Me). ^{19}F NMR (C_6D_5Br, 282.1 MHz, 293 K): −131.8 (d, ^3J 10.6 Hz, 2-C_6F_5), −161.8 (t, ^3J 21.2 Hz, 4-C_6F_5), −165.8 (app t, app ^3J 18.1 Hz, 3-C_6F_5).

NMR Tube Scale Synthesis of [Ti(N^{t}Bu)(Me_3[9]aneN$_3$)Cl]-[BAr^F_4] (8-BAr^F_4) from Ti(N^{t}Bu)(Me_3[9]aneN$_3$)Cl(Me) (5) or Ti(N^{t}Bu)(Me_3[9]aneN$_3$)Me_2 (1) and [Ph_3C][BAr^F_4] in CD_2Cl_2. Ti(N^{t}Bu)(Me_3[9]aneN$_3$)Cl(Me) (**5**, 0.005 g, 0.015 mmol) and $[Ph_3C]$-$[BAr^F_4]$ (0.014 g, 0.015 mmol) were dissolved in CD_2Cl_2 (0.75 mL). After 10 min the ^{1}H NMR showed quantitative conversion to **8-BAr^F_4** and Ph_3CMe. Alternatively, Ti(N^{t}Bu)(Me_3[9]aneN$_3$)Me_2 (**1**, 0.007 g, 0.020 mmol) and $[Ph_3C][BAr^F_4]$ (0.019 g, 0.020 mmol) were dissolved in CD_2Cl_2 (0.75 mL) to give quantitative conversion to **8-BAr^F_4** and Ph_3CMe. Subsequent addition of [PPN]Cl or pyridine to samples of $\mathbf{8}^+$ generated in this way showed quantitative conversion to **4** or $\mathbf{9}^+$, respectively. ^{1}H NMR (CD_2Cl_2, 499.9 MHz, 293 K): 4.00−2.30 (21H, br overlapping peaks, Me_3[9]aneN$_3$), 1.08 (9H, s, $NCMe_3$). A low-temperature ^{1}H spectrum recorded at 213 K showed a mixture of different species.

[Ti(N^{t}Bu)(Me_3[9]aneN$_3$)Cl(py)][BAr^F_4] (9-BAr^F_4). Ti(N^{t}Bu)-(Me_3[9]aneN$_3$)Cl(Me) (**5**, 0.11 g, 0.31 mmol) and $[Ph_3C][BAr^F_4]$ (0.29 g, 0.31 mmol) were dissolved in CH_2Cl_2 (10 mL) and stirred for 10 min. Pyridine (27.9 μL, 0.35 mmol) was added and the orange solution stirred for 16 h. The solution was concentrated to 5 mL, after which pentane was added with stirring, resulting in an orange precipitate. The supernatant was filtered off and the orange precipitate washed with pentane (3 × 5 mL) and dried in vacuo. Yield: 0.28 g (81%). Diffraction quality single crystals were obtained by slow diffusion of pentane into a CH_2Cl_2 solution. ^{1}H NMR (CD_2Cl_2, 299.9 MHz, 293 K): 9.20 (2H, dd, ^3J 6.6 Hz, ^4J 1.6 Hz, 2-NC_5H_5), 8.10 (1H, tt, ^3J 7.8 Hz, ^4J 1.5 Hz, 4-NC_5H_5), 7.68 (2H, app t, app ^3J 7.0 Hz, 3-NC_5H_5), 3.92 (1H, m, CH_2), 3.69 (1H, m, CH_2), 3.40 (3H, s, NMe), 3.40−2.60 (9H, overlapping m, CH_2), 3.29 (3H, s, NMe), 2.33 (1H, m, CH_2), 2.13 (3H, s, NMe), 0.98 (9H, s, $NCMe_3$). ^{13}C{^{1}H} NMR (CD_2Cl_2, 75.4 MHz, 293 K): 151.7 (2-NC_5H_5), 148.5 (br d, $^1J_{C-F}$ 241 Hz, 2-C_6F_5), 141.1 (4-NC_5H_5), 138.6 (br d, $^1J_{C-F}$ 247 Hz, 4-C_6F_5), 136.7 (br d, $^1J_{C-F}$ 250 Hz, 3-C_6F_5), 125.7 (3-NC_5H_5), 72.2 ($NCMe_3$), 58.1 (CH_2), 57.5 (CH_2), 56.3 (CH_2), 55.9 (CH_2), 55.5 (CH_2), 55.0 (CH_2), 54.4 (NMe), 54.2 (NMe), 48.9 (NMe), 30.7 ($NCMe_3$). ^{19}F NMR (CD_2Cl_2, 282.1 MHz, 293 K): −133.5 (d, ^3J 10.6 Hz, 2-C_6F_5), −164.0 (t, ^3J 20.4 Hz, 4-C_6F_5), −167.9 (app t, app ^3J 18.1 Hz, 3-C_6F_5). IR (NaCl plates, Nujol mull, cm^{-1}): 1644 (s), 1608 (w), 1514 (s), 1494 (w), 1276 (m), 1238 (s), 1084 (s), 1046 (w), 1000 (m), 980 (s), 774 (m), 756 (s), 704 (w), 682 (m), 660 (m). ES$^+$MS (MeCN): *m*/*z* 404.1 (12%) $[M]^+$, 325.1 (100%) $[M - C_5H_5N]^+$. Anal. Found (calcd for $C_{42}H_{35}BClF_{20}N_5Ti$): C 46.7 (46.5), H 3.2 (3.3), N 6.5 (6.5), Cl 3.3 (3.3).

[Ti_2(N^{t}Bu)$_2$(Me_3[9]aneN$_3$)$_2Me_2$(μ-Me)][BAr^F_4] (10-BAr^F_4). To a solution of Ti(N^{t}Bu)(Me_3[9]aneN$_3$)Me_2 (**1**, 0.069 g, 0.217 mmol) in C_6H_5Cl (1 mL) at −35 °C was added $[Ph_3C][BAr^F_4]$ (0.100 g, 0.108 mmol), resulting in a yellow solution. Hexane (4 mL) was added with stirring, resulting in a yellow oil. The mother liquor was decanted and the yellow oil triturated and washed with pentane (3 × 5 mL) to give **10-BAr^F_4** as a yellow powder, which was dried in vacuo. Yield: 0.090 g (64%). The cation is observed as a mixture of two diastereomers, hereafter referred to as isomer *A* and isomer *B*, in a 2.3:1 ratio. *Data for isomer "A"*: ^{1}H NMR (CD_2Cl_2, 500.0 MHz, 233 K): 3.50−2.60 (series of mutually overlapping m, some corresponding to isomer *B*, CH_2), 2.91 (6H, s, NMe), 2.88 (6H, s, NMe), 2.48 (6H, s, NMe), 1.12 (18H, s, $NCMe_3$), 0.26 (3H, s, TiMe bridging), −0.06 (6H, s, TiMe terminal). ^{13}C{^{1}H} NMR (CD_2Cl_2, 125.7 MHz, 233 K): 66.6 ($NCMe_3$), 56.7−54.8 (series of singlets overlapping with isomer *B*, CH_2), 52.7 (NMe), 51.8 (NMe), 48.7 (NMe), 32.3 ($NCMe_3$), 29.8 (TiMe terminal), 24.2 (TiMe bridging). *Data for isomer "B"*: ^{1}H NMR (CD_2Cl_2, 500.0 MHz, 233 K): 3.50−2.60 (series of mutually overlapping m, some corresponding to isomer *A*, CH_2), 2.90 (6H, s, NMe), 2.84 (6H, s, NMe), 2.59 (6H, s, NMe), 1.10 (18H, s, $NCMe_3$), 0.30 (3H, s, TiMe bridging), 0.04 (6H, s, TiMe terminal). ^{13}C{^{1}H} NMR (CD_2Cl_2, 125.7 MHz, 233 K): 66.8 ($NCMe_3$), 56.7−54.8 (series of singlets overlapping with isomer *A*, CH_2), 51.8 (NMe), 51.6 (NMe), 49.1 (NMe), 32.2 ($NCMe_3$), 30.0 (TiMe terminal), 22.8 (TiMe bridging). Data for $[B(C_6F_5)_4]^-$ anion: ^{13}C{^{1}H} NMR (CD_2Cl_2, 500.0 MHz, 233 K): 147.6 (br d, $^1J_{C-F}$ 247 Hz, 2-C_6F_5), 137.8 (br d, $^1J_{C-F}$ 225 Hz, 4-C_6F_5), 135.9 (br d, $^1J_{C-F}$ 247 Hz, 3-C_6F_5). ^{19}F NMR (CD_2Cl_2, 282.5 MHz, 293 K): −133.5 (d, ^3J 10.6 Hz, 2-C_6F_5), −164.0 (t, ^3J 20.4 Hz, 4-C_6F_5), −167.9 (app t, app ^3J 18.1 Hz, 3-C_6F_5). IR (NaCl plates, Nujol mull, cm^{-1}): 1643 (m), 1513 (s), 1351 (w), 1298 (w), 1275 (m), 1239 (s), 1206 (w), 1084 (s), 1005 (s), 980 (s), 891 (w), 776 (m), 756 (m), 684 (m), 661 (m). Anal. Found (calcd for $C_{53}H_{69}BF_{20}N_8Ti_2$): C 48.8 (48.8), H 5.2 (5.3), N 8.5 (8.6).

[Ti_2(N^{t}Bu)$_2$(Me_3[9]aneN$_3$)$_2Me_2$(μ-Cl)][BAr^F_4] (11-BAr^F_4). To a solution of Ti(N^{t}Bu)(Me_3[9]aneN$_3$)Cl(Me) (**5**, 0.037 g, 0.108 mmol) in CH_2Cl_2 (1 mL) was added $[Ph_3C][BAr^F_4]$ (0.100 g, 0.108 mmol). After 2 min Ti(N^{t}Bu)(Me_3[9]aneN$_3$)Me_2 (**1**, 0.035 g, 0.108 mmol) was added, resulting in a color change from orange to yellow. Pentane (4 mL) was added with stirring, resulting in an orange oil. The mother liquor was decanted and the yellow oil washed with pentane (3 × 5 mL). When a reduced pressure was applied to the oil, **11-BAr^F_4** was obtained as a yellow powder. Yield: 0.100 g (70%). Addition of [PPN]Cl (1 equiv) to a sample of **11-BAr^F_4** in CD_2Cl_2 re-formed **5**. The cation $\mathbf{11}^+$ is formed as a mixture of two diastereomers, hereafter referred to as isomer "*A*" and isomer "*B*", in a 2.5:1 ratio. *Data for isomer "A"*: ^{1}H NMR (CD_2Cl_2, 499.9 MHz, 253 K): 3.50−2.55 (series of mutually overlapping m, some corresponding to isomer *B*, CH_2), 3.06 (6H, s, NMe), 2.99 (6H, s, NMe), 2.52 (6H, s, NMe), 1.10 (18H, s, $NCMe_3$), 0.35 (6H, s, TiMe). ^{13}C{^{1}H} NMR (CD_2Cl_2, 125.7 MHz, 253 K): 67.7 ($NCMe_3$), 57.0 (CH_2), 56.0 (CH_2), 55.5 (CH_2), 55.3 (CH_2), 55.2 (CH_2), 54.7 (CH_2), 53.2 (NMe), 52.0 (NMe), 48.7

(NMe), 33.9 (TiMe), 31.7 (NC*Me*$_3$). *Data for isomer "B"*: ^{1}H NMR (CD_2Cl_2, 499.9 MHz, 253 K): 3.50−2.55 (series of mutually overlapping m, some corresponding to isomer *A*, CH_2), 3.04 (6H, s, NMe), 3.00 (6H, s, NMe), 2.56 (6H, s, NMe), 1.09 (18H, s, NCMe$_3$), 0.45 (3H, s, TiMe). ^{13}C{^{1}H} NMR (CD_2Cl_2, 125.7 MHz, 253 K): 68.0 (N*C*Me$_3$), 56.8 (CH_2), 56.2 (CH_2), 55.5 (CH_2), 55.4 (CH_2), 55.1 (CH_2), 54.4 (CH_2), 52.4 (NMe), 51.9 (NMe), 48.8 (NMe), 34.2 (TiMe), 31.8 (NC*Me*$_3$). Data for $[BAr^F_4]^-$ anion: ^{13}C{^{1}H} NMR (CD_2Cl_2, 125.7 MHz, 253 K): 148.0 (br d, $^1J_{C-F}$ 239 Hz, 2-C_6F_5), 138.2 (br d, $^1J_{C-F}$ 243 Hz, 4-C_6F_5), 136.3 (br d, $^1J_{C-F}$ 243 Hz, 3-C_6F_5). ^{19}F NMR (CD_2Cl_2, 282.1 MHz, 293 K): −133.5 (d, ^3J 10.6 Hz, 2-C_6F_5), −164.0 (t, ^3J 20.4 Hz, 4-C_6F_5), −167.9 (app t, app ^3J 18.1 Hz, 3-C_6F_5). IR (NaCl plates, Nujol mull, cm^{-1}): 1643 (m), 1513 (s), 1352 (m), 1297 (w), 1275 (m), 1241 (s), 1207 (w), 1086 (s), 1005 (s), 979 (s), 892 (w), 775 (m), 756 (m), 684 (m), 662 (m). Anal. Found (calcd for $C_{52}H_{66}BClF_{20}N_8Ti_2$): C 47.2 (47.1), H 4.9 (5.0), N 8.4 (8.5).

NMR Tube Scale Reaction of Ti(N^{t}Bu)(Me$_3$[9]aneN$_3$)(CH$_2$SiMe$_3$)$_2$ (2) with [PhNMe$_2$][BAr$^F_4$] (1 equiv). Ti(N^{t}Bu)(Me$_3$[9]aneN$_3$)(CH$_2$SiMe$_3$)$_2$ (**2**, 0.007 g, 0.015 mmol) and [PhNMe$_2$H][BAr$^F_4$] (0.012 g, 0.015 mmol) were dissolved in CD_2Cl_2 (0.75 mL). The ^{1}H NMR spectrum showed a 1:1 mixture of Ti(N^{t}Bu)(Me$_3$[9]aneN$_3$)Cl$_2$ (**4**) and Ti(N^{t}Bu)(Me$_3$[9]aneN$_3$)(CH$_2$SiMe$_3$)$_2$ (**2**) along with resonances attributable to [PhNMe$_2$(CD$_2$Cl)][BAr$^F_4$] (**12-*d*$_2$-BAr$^F_4$**) and SiMe$_4$. ES$^+$MS (MeCN) for **12**$^+$-***d*$_2$**: *m*/*z* 172.1 (100%) [M]$^+$.

Reaction of Ti(N^{t}Bu)(Me$_3$[9]aneN$_3$)(CH$_2$SiMe$_3$)$_2$ (2) with [PhNMe$_2$H][BAr$^F_4$] (2 equiv). To a stirred solution of Ti(N^{t}Bu)(Me$_3$[9]aneN$_3$)(CH$_2$SiMe$_3$)$_2$ (**2**, 0.20 g, 0.43 mmol) in CH_2Cl_2 (10 mL) at 0 °C was added [PhNMe$_2$H][BAr$^F_4$] (0.69 g, 0.86 mmol) in CH_2Cl_2 (20 mL). The orange solution was allowed to warm to room temperature and stirred for a further 16 h. The solution was concentrated to approximately 10 mL, then hexane (10 mL) was added with stirring to give an orange oil. The oil was redissolved in CH_2Cl_2 (3 mL) and carefully layered with hexane. After 10 days colorless diffraction-quality crystals of [PhNMe$_2$(CH$_2$Cl)][BAr$^F_4$] (**12-BAr$^F_4$**) had formed, which were filtered off and dried in vacuo. Yield: 0.137 g (37%). ^{1}H NMR (CD_2Cl_2, 499.9 MHz, 293 K): 7.74−7.70 (3H, overlapping m, 2- and 4-C_6H_5), 7.58 (2H, m, 3-C_6H_5), 5.25 (2H, s, CH_2Cl), 3.67 (6H, s, NMe_2). ^{13}C{^{1}H} NMR (CD_2Cl_2, 125.7 MHz, 293 K): 148.4 (br d, $^1J_{C-F}$ 244 Hz, 2-C_6F_5), 138.7 (br d, $^1J_{C-F}$ 246 Hz, 4-C_6F_5), 136.6 (br d, $^1J_{C-F}$ 246 Hz, 3-C_6F_5), 132.8 (4-C_6H_5), 132.0 (2-C_6H_5), 120.0 (3-C_6H_5), 74.0 (CH_2Cl), 54.0 (NMe_2). ^{19}F NMR (CD_2Cl_2, 282.4 MHz, 293 K): −133.5 (d, ^3J 10.6 Hz, 2-C_6F_5), −164.0 (t, ^3J 20.4 Hz, 4-C_6F_5), −167.9 (app t, app ^3J 18.1 Hz, 3-C_6F_5). ES$^+$MS (MeCN): *m*/*z* 170.1 (100%) [M]$^+$.

NMR Tube Scale Reaction of [Ti(N^{t}Bu)(Me$_3$[9]aneN$_3$)(CH$_2$SiMe$_3$)][BAr$^F_4$] (7-BAr$^F_4$) with PhNMe$_2$. To a solution of **7-BAr$^F_4$** {generated in situ from Ti(N^{t}Bu)(Me$_3$[9]aneN$_3$)(CH$_2$SiMe$_3$)$_2$ (**2**, 0.010 g, 0.022 mmol) and [Ph$_3$C][BAr$^F_4$] (0.020 g, 0.022 mmol)} in CD_2Cl_2 (0.75 mL) was added PhNMe$_2$ (2.7 μL, 0.022 mmol). After 10 min the ^{1}H NMR spectrum showed quantitative conversion to **13** along with resonances for **12-*d*$_2$-BAr$^F_4$** and unreacted PhNMe$_2$.

NMR Tube Scale Reaction of Ti(N^{t}Bu)(Me$_3$[9]aneN$_3$)Cl(CH$_2$SiMe$_3$) (3) with [PhNMe$_2$H][BAr$^F_4$]. Ti(N^{t}Bu)(Me$_3$[9]aneN$_3$)Cl(CH$_2$SiMe$_3$) (**3**, 0.007 g, 0.017 mmol) and [PhNMe$_2$H][BAr$^F_4$] (0.014 g, 0.017 mmol) were dissolved in CD_2Cl_2 (0.75 mL). After 10 min an ^{1}H NMR spectrum showed a mixture of products. After 16 h the ^{1}H NMR spectrum showed quantitative conversion to **4** and **12-*d*$_2$-BAr$^F_4$**.

NMR Tube Scale Reaction of [Ti(N^{t}Bu)(Me$_3$[9]aneN$_3$)Cl][BAr$^F_4$] (8-BAr$^F_4$) with PhNMe$_2$. To a solution of **8-BAr$^F_4$** {generated in situ from Ti(N^{t}Bu)(Me$_3$[9]aneN$_3$)Cl(Me) (**5**, 0.006 g, 0.017 mmol) and [Ph$_3$C][BAr$^F_4$] (0.016 g, 0.017 mmol)} in CD_2Cl_2 (0.75 mL) was added PhNMe$_2$ (2.2 μL, 0.017 mmol). After 16 h the ^{1}H NMR spectrum showed quantitative conversion to **4** and **12-*d*$_2$-BAr$^F_4$**.

NMR Tube Scale Synthesis of [Ti$_2$(N^{t}Bu)$_2$(Me$_3$[9]aneN$_3$)$_2$(CH$_2$SiMe$_3$)$_2$(μ-Cl)][BAr$^F_4$] (13-BAr$^F_4$). To a solution of **7-BAr$^F_4$** {generated in situ from Ti(N^{t}Bu)(Me$_3$[9]aneN$_3$)(CH$_2$SiMe$_3$)$_2$ (**2**, 0.0050 g, 0.011 mmol) and [Ph$_3$C][BAr$^F_4$] (0.0099 g, 0.011 mmol)} in CD_2Cl_2 (0.75 mL) was added Ti(N^{t}Bu)(Me$_3$[9]aneN$_3$)Cl(CH$_2$SiMe$_3$) (**3**, 0.0044 g, 0.011 mmol), resulting in a bright orange solution. After 10 min an ^{1}H NMR spectrum was recorded, which showed quantitative conversion to **11-BAr$^F_4$**. Addition of [PPN]Cl (1 equiv) to solutions of **13**$^+$ forms **3** quantitatively. The cation **13**$^+$ is a mixture of isomers. ^{1}H NMR (CD_2Cl_2, 499.9 MHz, 203 K): 3.7−2.2 (48H, series of mutually overlapping m, NCH_2), 3.09 (6H, s, NMe), 2.99 (12H, 2 × overlapping s, NMe), 2.95 (6H, s, NMe), 2.52 (6H, s, NMe), 2.38 (6H, s, NMe), 1.14 (4H, app d, app ^2J 9.3 Hz, C*H*$_a$H$_b$SiMe$_3$), 1.05 (36H, 2 × overlapping s, NCMe$_3$), 0.53 (2H, d, ^2J 8.8 Hz, CH$_a$*H*$_b$SiMe$_3$), 0.33 (2H, d, ^2J 9.3 Hz, CH$_a$*H*$_b$SiMe$_3$), −0.02 (18H, s, CH$_2$Si*Me*$_3$), −0.05 (18H, s, CH$_2$Si*Me*$_3$). ^{13}C{^{1}H} NMR (CD_2Cl_2, 125.7 MHz, 203 K): 147.2 (br d, $^1J_{C-F}$ 244 Hz, 2-C_6F_5), 137.5 (br d, $^1J_{C-F}$ 242 Hz, 4-C_6F_5), 135.5 (br d, $^1J_{C-F}$ 244 Hz, 3-C_6F_5), 68.3 (N*C*Me$_3$), 68.2 (N*C*Me$_3$), 55.7 (NMe), 53.2 (NMe), 51.9 (2 × NMe), 49.1 (NMe), 48.8 (NMe), 31.8 (NC*Me*$_3$), 31.7 (NC*Me*$_3$), 3.3 (SiMe$_3$), 3.1 (SiMe$_3$). The CH_2 resonances were too broad to be observed in a ^{13}C spectrum or DEPT-135. ^{19}F NMR (CD_2Cl_2, 282.4 MHz, 293 K): −133.5 (d, ^3J 10.6 Hz, 2-C_6F_5), −164.0 (t, ^3J 20.4 Hz, 4-C_6F_5), −167.9 (app t, app ^3J 18.1 Hz, 3-C_6F_5). ^{29}Si NMR (HMQC ^{1}H-observed, CD_2Cl_2, 299.9 MHz, 293 K): −1.8 (CH_2SiMe_3).

[Ti(N^{t}Bu)(Me$_3$[9]aneN$_3$)Me(Ph$_3$PO)][MeBAr$^F_3$] (14-MeBAr$^F_3$). To a solution of Ti(N^{t}Bu)(Me$_3$[9]aneN$_3$)Me$_2$ (**1**, 0.050 g, 0.156 mmol) in C_6H_5Cl (2 mL) was added BAr$^F_3$ (0.080 g, 0.156 mmol) in C_6H_5Cl (2 mL). After 5 min a solution of Ph_3PO (0.043 g, 0.156 mmol) in C_6H_5Cl (2 mL) was added, resulting in a color change from orange to yellow. The volatiles were removed under reduced pressure to give **14-MeBAr$^F_3$** as an orange oil containing 1 equiv of C_6H_5Cl per titanium. Yield: 0.150 g (80%). ^{1}H NMR (C_6D_5Br, 299.9 MHz, 293 K): 7.57 (6H, dd, $^3J_{P-H}$ 12.9 Hz, $^3J_{H-H}$ 6.9 Hz, 2-PPh_3), 7.27 (3H, m, 4-PPh_3), 7.21 (6H, m, 3-PPh_3), 2.86 (2H, m, CH_2), 2.73 (2H, m, CH_2 ring), 2.65 (3H, s, NMe), 2.35 (3H, s, NMe), 2.23−1.70 (8H, overlapping m, CH_2), 1.56 (3H, s, NMe), 1.04 (3H, br s, BMe), 0.93 (9H, s, NCMe$_3$), 0.30 (3H, s, TiMe). ^{13}C{^{1}H} NMR (C_6D_5Br, 75.4 MHz, 293 K): 149.0 (br d, $^1J_{C-F}$ 243 Hz, 2-C_6F_5), 137.9 (br d, $^1J_{C-F}$ 243 Hz, 4-C_6F_5), 136.2 (br d, $^1J_{C-F}$ 243 Hz, 3-C_6F_5), 134.1 (4-C_6H_5), 133.1 (d, $^2J_{C-P}$ 11.4 Hz, 2-C_6H_5), 129.2 (d, obscured by solvent resonance, 3-C_6H_5), 67.7 (N*C*Me$_3$), 56.7 (CH_2), 56.3 (NMe), 55.1 (CH_2), 54.8 (overlapping NMe and CH_2), 53.9 (NMe), 53.1 (CH_2), 51.4 (CH_2), 47.3 (CH_2), 32.5 (NC*Me*$_3$), 31.4 (TiMe). ^{19}F NMR (C_6D_5Br, 282.1 MHz, 293 K): −132.1 (d, ^3J 20.0 Hz, 2-C_6F_5), −164.2 (t, ^3J 21.2 Hz, 4-C_6F_5), −166.7 (app t, app ^3J 20.0 Hz, 3-C_6F_5). ^{31}P{^{1}H} NMR (C_6D_5Br, 121.4 MHz, 293 K): 44.9 (PPh_3). IR (NaCl plates, thin film, cm^{-1}): 3064 (m), 2965 (s), 2920 (s), 2865 (s), 2360 (w), 2342 (w), 1640 (s), 1591 (m), 1511 (s), 1454 (br s), 1383 (m), 1366 (m), 1354 (m), 1298 (m), 1268 (s), 1236 (s), 1206 (m), 1140 (br s), 1084 (br s), 999 (br s), 935 (s), 893 (w), 841 (m), 803 (m), 782 (m), 746 (s), 727 (s), 696 (s), 660 (m), 643 (w). ES$^+$MS (MeCN): *m*/*z* 583.3 (40%) [M]$^+$, 172.2 (100%) [Me$_3$[9]aneN$_3$H]$^+$. ES$^+$-HRMS (MeCN): *m*/*z* found (calcd for $C_{32}H_{48}N_4OPTi$, [M]$^+$) 583.3025 (538.3045). Anal. Found (calcd for $C_{51}H_{51}BF_{15}N_4OPTi\cdot C_6H_5Cl$): C 55.2 (55.5), H 4.7 (4.7), N 4.2 (4.5).

[Ti(N^{t}Bu)(Me$_3$[9]aneN$_3$)(CH$_2$SiMe$_3$)(Ph$_3$PO)][BAr$^F_4$] (13-BAr$^F_4$). To a solution of Ti(N^{t}Bu)(Me$_3$[9]aneN$_3$)(CH$_2$SiMe$_3$)$_2$ (**2**, 0.050 g, 0.108 mmol) in CH_2Cl_2 (2 mL) was added [Ph$_3$C][BAr$^F_4$] (0.100 g, 0.108 mmol) in CH_2Cl_2 (2 mL). After 5 min Ph_3PO (0.030 g, 0.108 mmol) was added, resulting in a color change from orange to yellow. The solution was concentrated to approximately 1 mL, after which hexane (2 mL) was added, resulting in a yellow oil.

The mother liquor was decanted away and the oil washed with hexane (3 × 2 mL). When a reduced pressure was applied to the oil, a yellow powder was obtained, which contained 0.33 equiv of hexane per titanium by ^{1}H NMR. Yield: 0.101 g (69%). ^{1}H NMR (CD_2Cl_2, 499.9 MHz, 293 K): 7.83 (6H, m, 2-PPh_3), 7.76 (3H, m, 4-PPh_3), 7.62 (6H, m, 3-PPh_3), 3.45 (1H, m, NCH_2), 3.34 (1H, m, NCH_2), 3.15 (3H, s, NMe), 2.95−2.75 (2H, overlapping m, NCH_2), 2.82 (3H, s, NMe), 2.63 (2H, overlapping m, NCH_2), 2.53 (2H, overlapping m, NCH_2), 2.50−2.32 (4H, overlapping m, NCH_2), 2.07 (3H, s, NMe), 1.12 (9H, s, $NCMe_3$), 0.95 (1H, d, ^2J 10.2 Hz, $CH_aH_bSiMe_3$), 0.10 (1H, d, ^2J 10.2 Hz, $CH_aH_bSiMe_3$), 0.04 (9H, s, CH_2SiMe_3). ^{13}C{^{1}H} NMR (CD_2Cl_2, 125.7 MHz, 293 K): 148.5 (br d, $^1J_{C-F}$ 244 Hz, 2-C_6F_5), 138.6 (br d, $^1J_{C-F}$ 246 Hz, 4-C_6F_5), 136.8 (br d, $^1J_{C-F}$ 246 Hz, 3-C_6F_5), 134.5 (d, $^4J_{C-P}$ 2.7 Hz, 4-C_6H_5), 133.6 (d, $^2J_{C-P}$ 11.4 Hz, 2-C_6H_5), 129.7 (d, $^3J_{C-P}$ 6.1 Hz, 3-C_6H_5), 69.4 ($NCMe_3$), 57.7 (CH_2), 56.9 (CH_2), 56.2 (CH_2), 56.0 (CH_2), 55.1 (CH_2), 54.0 (CH_2), 53.7 (NMe), 52.2 (NMe), 50.0 (CH_2SiMe_3), 48.9 (NMe), 33.1 ($NCMe_3$), 4.1 ($SiMe_3$). ^{19}F NMR (CD_2Cl_2, 282.1 MHz, 293 K): −133.5 (d, ^3J 10.6 Hz, 2-C_6F_5), −164.0 (t, ^3J 20.4 Hz, 4-C_6F_5), −167.9 (app t, app ^3J 18.1 Hz, 3-C_6F_5). ^{31}P{^{1}H} NMR (CD_2Cl_2, 121.5 MHz, 293 K): 43.4 (PPh_3). ^{29}Si NMR (HMQC ^{1}H-observed, CD_2Cl_2, 299.9 MHz, 293 K): −0.7 (CH_2SiMe_3). IR (NaCl plates, Nujol mull, cm^{-1}): 1643 (m), 1592 (w), 1513 (s), 1412 (w), 1354 (w), 1299 (w), 1275 (m), 1231 (m), 1205 (w), 1141 (s), 1121 (s), 1086 (s), 1007 (m), 980 (s), 907 (m), 849 (m), 820 (m), 775 (m), 755 (m), 726 (s), 695 (m), 684 (m), 662 (m). Anal. Found (calcd for $C_{59}H_{56}BF_{20}N_4OPSiTi\cdot 0.33C_6H_{14}$): C 53.9 (53.7), H 4.6 (4.5), N 4.1 (4.1).

[Ti(N^{t}Bu)(Me$_3$[9]aneN$_3$)Me(py)][BAr$^F_4$] (16-BAr$^F_4$). To a stirred solution of Ti(N^{t}Bu)(Me$_3$[9]aneN$_3$)Me$_2$ (**1**, 0.050 g, 0.156 mmol) and pyridine (14.0 μL, 0.172 mmol) in CH_2Cl_2 (2 mL) at −78 °C was added [Ph_3C][BAr$^F_4$] (0.144 g, 0.156 mmol) in CH_2Cl_2 (2 mL). The resulting light yellow solution was concentrated to approximately 1 mL, after which hexane (5 mL) was added with stirring, resulting in a bright yellow precipitate. The precipitate was filtered off and dried in vacuo. Yield: 0.086 g (52%). ^{1}H NMR (CD_2Cl_2, 299.9 MHz, 213 K): 8.75 (2H, d, ^3J 6.5 Hz, 2-NC_5H_5), 8.00 (1H, t, ^3J 7.6 Hz, 4-NC_5H_5), 7.58 (2H, app t, app ^3J 6.5 Hz, 3-NC_5H_5), 3.49 (2H, overlapping m, CH_2), 3.09 (3H, s, NMe), 3.02 (3H, s, NMe), 3.15−2.62 (8H, overlapping m, CH_2), 2.50 (1H, m, CH_2), 2.45 (3H, s, NMe), 2.34 (1H, m, CH_2), 1.01 (9H, s, $NCMe_3$), 0.46 (3H, s, TiMe). ^{13}C{^{1}H} NMR (CD_2Cl_2, 75.4 MHz, 213 K): 150.4 (2-NC_5H_5), 147.5 (br d, $^1J_{C-F}$ 240 Hz, 2-C_6F_5), 139.9 (4-NC_5H_5), 137.7 (br d, $^1J_{C-F}$ 242 Hz, 4-C_6F_5), 135.8 (br d, $^1J_{C-F}$ 245 Hz, 3-C_6F_5), 124.7 (3-NC_5H_5), 68.4 ($NCMe_3$), 55.6 (CH_2), 55.5 (2 x CH_2), 55.4 (CH_2), 54.4 (CH_2), 54.3 (CH_2), 52.9 (NMe), 52.3 (NMe), 49.1 (NMe), 34.9 (TiMe), 30.9 ($NCMe_3$). ^{19}F NMR (CD_2Cl_2, 282.1 MHz, 213 K): −133.9 (d, ^3J 10.6 Hz, 2-C_6F_5), −163.1 (t, ^3J 20.4 Hz, 4-C_6F_5), −167.1 (app t, app ^3J 18.1 Hz, 3-C_6F_5). IR (NaCl plates, Nujol mull, cm^{-1}): 1643 (m), 1607 (w), 1514 (s), 1354 (w), 1298 (w), 1277 (m), 1245 (m), 1209 (w), 1084 (s), 1002 (m), 979 (s), 775 (m), 757 (m), 707 (w), 683 (m), 661 (m). Anal. Found (calcd for $C_{43}H_{38}BF_{20}N_5Ti$): C 48.4 (48.6), H 3.8 (3.6), N 6.4 (6.6).

[Ti(N^{t}Bu)(Me$_3$[9]aneN$_3$)(NC$_5$H$_4$)][BAr$^F_4$] (17-BAr$^F_4$). To a solution of Ti(N^{t}Bu)(Me$_3$[9]aneN$_3$)(CH_2SiMe_3)$_2$ (**2**, 0.100 g, 0.215 mmol) in CH_2Cl_2 (1 mL) was added [Ph_3C][BAr$^F_4$] (0.198 g, 0.215 mmol) in CH_2Cl_2 (1 mL). Pyridine (17.4 μL, 0.015 mmol) was added, resulting in a color change from orange to yellow. Pentane (5 mL) was added with stirring, resulting in a yellow oil. The supernatant was decanted and the yellow oil washed with pentane (3 × 2 mL). When a reduced pressure was applied to the oil, a yellow powder was obtained. Yield: 0.148 g (66%). The corresponding NMR tube scale reaction of **7-BAr$^F_4$** in CH_2Cl_2 with pyridine-d_5 afforded [Ti(N^{t}Bu)(Me$_3$[9]aneN$_3$)(NC$_5$D$_4$)][BAr$^F_4$] (**17-d_4-BAr$^F_4$**) and $SiMe_4$-d_1, which showed the expected ^{2}H NMR resonances. ^{1}H NMR (CD_2Cl_2, 299.9 MHz, 313 K): 8.50 (1H, dt, ^3J 5.3 Hz, ^4J 1.2 Hz, 6-NC_5H_4), 7.97 (1H, dt, ^3J 7.6 Hz, ^4J 1.2 Hz, 3-NC_5H_4), 7.75 (1H, td, ^3J 7.6 Hz, ^4J 1.2 Hz, 4-NC_5H_4), 7.35 (1H, ddd, ^3J 7.6 Hz, 5.3 Hz, ^4J 1.2 Hz, 5-NC_5H_4), 3.07 (6H, m, CH_2), 2.94 (6H, m, CH_2), 2.60 (9H, br s, NMe), 0.79 (9H, s, $NCMe_3$). ^{13}C{^{1}H} NMR (CD_2Cl_2, 75.4 MHz, 313 K): 212.4 (2-NC_5H_4), 151.9 (6-NC_5H_4), 148.5 (br d, $^1J_{C-F}$ 241 Hz, 2-C_6F_5), 145.2, 141.2 (3- and 4-NC_5H_4), 138.6 (br d, $^1J_{C-F}$ 247 Hz, 4-C_6F_5), 136.7 (br d, $^1J_{C-F}$ 250 Hz, 3-C_6F_5), 131.7 (5-NC_5H_4), 69.3 ($NCMe_3$), 55.8 (CH_2 ring), 50.8 (NMe), 31.8 ($NCMe_3$). ^{19}F NMR (CD_2Cl_2, 282.4 MHz, 293 K): −133.5 (d, ^3J 10.6, 2-C_6F_5), −164.0 (t, ^3J 20.4 Hz, 4-C_6F_5), −167.9 (app t, app ^3J 18.1 Hz, 3-C_6F_5). IR (NaCl plates, Nujol mull, cm^{-1}): 1643 (s), 1605 (m), 1514 (s), 1275 (s), 1244 (m), 1155 (w), 1088 (s), 979 (s), 863 (m), 775 (s), 757 (s), 725 (w), 705 (m), 684 (s), 662 (s). A satisfactory elemental analysis could not be obtained.

Table 4. X-ray Data Collection and Processing Parameters for [Ti(N^{t}Bu)(Me$_3$[9]aneN$_3$)Cl(py)][BAr$^F_4$] (9-BAr$^F_4$) and [PhNMe$_2$(CH$_2$Cl)][BAr$^F_4$] (12-BAr$^F_4$)

	9-BAr$^F_4$	12-BAr$^F_4$
empirical formula	$C_{42}H_{35}BClF_{20}N_5Ti$	$C_{33}H_{13}BClF_{20}N$
fw	1083.90	849.70
temp/K	150	150
wavelength/Å	0.71073	0.71073
space group	$P2_1/c$	$Pbca$
a/Å	13.1935(2)	13.8835(2)
b/Å	21.1046(3)	18.8229(3)
c/Å	15.6878(3)	24.5280(5)
α/deg	90	90
β/deg	90.9546(8)	90
γ/deg	90	90
V/Å^3	4367.6(1)	6409.8(2)
Z	4	8
d(calcd)/Mg·m^{-3}	1.648	1.761
abs coeff/mm^{-1}	0.383	0.265
R indices [$I > 3\sigma(I)$][a]	$R_1 = 0.0580$	0.0372
	$R_w = 0.0680$	0.0396

[a] $R_1 = \sum||F_o| - |F_c||/\sum|F_o|$; $R_w = \sqrt{\{\sum w(|F_o| - |F_c|)^2/\sum(w|F_o|^2\}}$.

Crystal Structure Determinations of [Ti(N^{t}Bu)(Me$_3$[9]aneN$_3$)Cl(py)][BAr$^F_4$] (9-BAr$^F_4$) and [PhNMe$_2$(CH$_2$Cl)][BAr$^F_4$] (12-BAr$^F_4$). Crystal data collection and processing parameters are given in Table 4. Crystals were mounted on a glass fiber using perfluoropolyether oil and cooled rapidly to 150 K in a stream of cold N_2 using an Oxford Cryosystems CRYOSTREAM unit. Diffraction data were measured using an Enraf-Nonius KappaCCD diffractometer. Intensity data were processed using the DENZO-SMN package.[110] The structures were solved using the direct-methods program SIR92,[111] which located all non-hydrogen atoms. Subsequent full-matrix least-squares refinement was carried out using the CRYSTALS program suite.[112] Coordinates and anisotropic thermal parameters of all non-hydrogen atoms were refined. Disorder of the CH_2CH_2 linkages in the Me$_3$[9]aneN$_3$ ring of **9**$^+$ was satisfactorily modeled. Hydrogen atoms were positioned geometrically. Full listings of atomic coordinates, bond lengths and angles, and displacement parameters have been deposited at the Cambridge Crystallographic Data Center. See Guidelines for Authors, Issue No. 1.

Computational Details. All the calculations have been performed with the Gaussian03 package[113] at the B3PW91 level.[114,115] The titanium atom was represented by the relativistic effective core potential (RECP) from the Stuttgart group (12 valence electrons) and its associated basis set,[116] augmented by an f polarization function (α = 0.869).[117] The silicon atom was represented by RECP

(110) Otwinowski, Z.; Minor, W. *Processing of X-ray Diffraction Data Collected in Oscillation Mode*; Academic Press: New York, 1997.

(111) Altomare, A.; Cascarano, G.; Giacovazzo, G.; Guagliardi, A.; Burla, M. C.; Polidori, G.; Camalli, M. *J. Appl. Crystallogr.* **1994**, *27*, 435.

(112) Betteridge, P. W.; Cooper, J. R.; Cooper, R. I.; Prout, K.; Watkin, D. J. *J. Appl. Crystallogr.* **2003**, *36*, 1487.

from the Stuttgart group and the associated basis set,[118] augmented by a d polarization function.[119] The remaining atoms (C, H, N) were represented by a 6-31G(d,p) basis set.[120] Full optimizations of geometry without any constraint were performed, followed by analytical computation of the Hessian matrix to confirm the nature of the located extrema as minima or transition states on the potential energy surface. The nature of the transition states was checked by slightly perturbing the TS geometry along the TS vector in both directions and optimizing the resulting geometries as local minima to ensure the nature of the connected intermediates. NMR chemical shifts and J_{CH} coupling constants were computed using the GIAO method[121,122] at the B3PW91 level. For the NMR parameters, all electron calculations were considered where the basis set for Ti was the TZP basis set of Ahlrichs,[123] and all the other atoms were described with the IGLOO-II basis set.[124] Natural bonding orbital analysis[125] was performed as implemented in Gaussian03.

Acknowledgment. We thank the EPSRC, DSM Research BV, SABIC EuroPetrochemicals, Millennium Pharmaceuticals, CNRS, and the British Council for support, and Professor G. I. Nikonov and Dr. N. H. Rees for technical assistance and helpful discussions.

Supporting Information Available: X-ray crystallographic files in CIF format for the structure determinations of [Ti(N^{t}Bu)(Me$_3$[9]aneN$_3$)Cl(py)][BAr$^F{}_4$] (**9-BAr$^F{}_4$**) and [PhNMe$_2$(CH$_2$Cl)][BAr$^F{}_4$] (**12-BAr$^F{}_4$**), and further details of the DFT calculations. This material is available free of charge via the Internet at http://pubs.acs.org.

OM060096R

(113) Frisch, M. J.; Trucks, G. W.; Schlegel, H. B.; Scuseria, G. E.; Robb, M. A.; Cheeseman, J. R.; Montgomery, J. A., Jr.; Vreven, T.; Kudin, K. N.; Burant, J. C.; Millam, J. M.; Iyengar, S. S.; Tomasi, J.; Barone, V.; Mennucci, B.; Cossi, M.; Scalmani, G.; Rega, N.; Petersson, G. A.; Nakatsuji, H.; Hada, M.; Ehara, M.; Toyota, K.; Fukuda, R.; Hasegawa, J.; Ishida, M.; Nakajima, T.; Honda, Y.; Kitao, O.; Nakai, H.; Klene, M.; Li, X.; Knox, J. E.; Hratchian, H. P.; Cross, J. B.; Bakken, V.; Adamo, C.; Jaramillo, J.; Gomperts, R.; Stratmann, R. E.; Yazyev, O.; Austin, A. J.; Cammi, R.; Pomelli, C.; Ochterski, J. W.; Ayala, P. Y.; Morokuma, K.; Voth, G. A.; Salvador, P.; Dannenberg, J. J.; Zakrzewski, V. G.; Dapprich, S.; Daniels, A. D.; Strain, M. C.; Farkas, O.; Malick, D. K.; Rabuck, A. D.; Raghavachari, K.; Foresman, J. B.; Ortiz, J. V.; Cui, Q.; Baboul, A. G.; Clifford, S.; Cioslowski, J.; Stefanov, B. B.; Liu, G.; Liashenko, A.; Piskorz, P.; Komaromi, I.; Martin, R. L.; Fox, D. J.; Keith, T.; Al-Laham, M. A.; Peng, C. Y.; Nanayakkara, A.; Challacombe, M.; Gill, P. M. W.; Johnson, B.; Chen, W.; Wong, M. W.; Gonzalez, C.; Pople, J. A. *Gaussian 03, Revision C.02*; Gaussian, Inc.: Wallingford, CT, 2004.

(114) Becke, A. D. *J. Chem. Phys.* **1993**, *98*, 5648.

(115) Perdew, J. P.; Wang, Y. *Phys. Rev. B* **1992**, *45*, 13244.

(116) Andrae, D.; Haussermann, U.; Dolg, M.; Stoll, H.; Preuss, H. *Theor. Chim. Acta* **1990**, *77*, 123.

(117) Ehlers, A. W.; Bohme, M.; Dapprich, S.; Gobbi, A.; Hollwarth, A.; Jonas, V.; Kohler, K. F.; Stegmann, R.; Veldkamp, A.; Frenking, G. *Chem. Phys. Lett.* **1993**, *208*, 111.

(118) Bergner, A.; Dolg, M.; Kuchle, W.; Stoll, H.; Preuss, H. *Mol. Phys.* **1993**, *30*, 1431.

(119) Hollwarth, A.; Bohme, H.; Dapprich, S.; Ehlers, A. W.; Gobbi, A.; Jonas, V.; Kohler, K. F.; Stagmann, R.; Veldkamp, A.; Frenking, G. *Chem. Phys. Lett.* **1993**, *203*, 237.

(120) Hariharan, P. C.; Pople, J. A. *Theor. Chim. Acta* **1973**, *28*, 213.

(121) Lee, A. M.; Handy, N. C.; Colwell, S. M. *J. Chem. Phys.* **1995**, *103*, 10095.

(122) Ditchfiled, R. J. *Chem. Phys. Lett.* **1972**, *56*, 5688.

(123) Schäfer, A.; Huber, C.; Ahlrichs, R. J. *Chem. Phys. Lett.* **1994**, *100*, 5829.

(124) Kutzelnigg, W.; Fleischer, U.; Schindler, M. *IGLOO-II*; Springer-Verlag: Berlin, 1990.

(125) Reed, A. E.; Curtiss, L. A.; Weinhold, F. *Chem. Rev.* **1988**, *88*, 899.